Identification of Differentially Expressed Nucleolar TGF-β1 Target (DENTT) in Human Lung Cancer Cells That Is a New Member of the TSPY/SET/NAP-1 Superfamily

Laurent L. Ozbun, Liang You,[1] Sharon Kiang, Jerry Angdisen,
Alfredo Martinez, and Sonia B. Jakowlew[2]

Department of Cell and Cancer Biology, National Cancer Institute, Medicine Branch, Rockville, Maryland 20850

The transforming growth factor-β1 (TGF-β1) responsive epithelial non-small-cell lung cancer (NSCLC) cell line NCI-H727 was used to identify potential target genes involved in TGF-β1-mediated responses. Comparative cDNA expression patterns between cells treated with TGF-β1 and those treated with vehicle were generated by differential mRNA display. One 496-bp fragment, differentially increased threefold by TGF-β1 and hybridizing to a 2.7-kb mRNA species in NCI-H727 cells by Northern analysis, revealed no significant match to any known gene sequence. The mRNA transcript of this novel gene that we named differentially expressed nucleolar TGF-β1 target (DENTT) is expressed in several normal human tissues, with the highest level of expression in brain. Human brain cDNA library screening and 5′ rapid amplification of cDNA ends yielded full-length DENTT cDNA containing an 1899-bp open reading frame encoding a predicted 633-amino-acid protein with four potential nuclear localization signals (NLSs) and two coiled-coil regions. DENTT contains a conserved 191-residue domain that shows significant identity to, and defines, the TSPY/TSPY-like/SET/NAP-1 superfamily. Enhanced green fluorescent protein (EGFP)-tagged full-length DENTT transfected into COS-7 cells showed nucleolar and cytoplasmic localization. Transfection of EGFP-tagged DENTT NLS deletion constructs lacking the bipartite NLS-1 were excluded from the nucleolus. While NLS-1 is necessary for nucleolar localization of DENTT, it is not sufficient for sole nucleolar localization. Our data show that DENTT mRNA induction by TGF-β1 correlates with induction of TGF-β1 mRNA, induction of extracellular matrix gene expression, and inhibition of colony formation in soft agarose in TGF-β1 responsive NSCLC cells when exposed to TGF-β1. TGF-β1 does not induce DENTT mRNA expression in TGF-β1 nonresponsive NSCLC cells. Our data suggest that this novel TGF-β1 target gene has distinct domains for direction to different subnuclear locations. © 2001 Academic Press

INTRODUCTION

Lung cancer has become the leading cause of cancer mortality among both men and women in the United States, accounting for 28% of all cancer deaths in 1998 (Landis *et al.,* 1999). The peripheral location and late presentation of many lung cancers prevent extensive analysis of the early molecular events associated with these cancers. Most lung cancers are usually diagnosed at a time that is too late for effective treatment, and the therapeutic procedures that are currently available to treat lung cancer are not adequate to make an effective impact on this disease. Despite advances in cytotoxic drug development, radiotherapy, and patient management, the 5-year survival rate for lung cancer is less than 14% and has shown little improvement over the past 30 years (Ginsberg, 1993). An important step toward determining key intervention points for lung cancer is a clear understanding of the molecular pathogenesis of this disease. Little information is known about the sequence of genetic events leading to lung cancer. Present theories suggest that as many as 10–20 events, including alterations of oncogenes and tumor suppressor genes, have occurred by the time lung cancer becomes clinically evident. Although putative oncogenes and tumor suppressor genes, including ras, myc, Bcl-2, c-erb-B2, Rb, p53, and p16^{INK4A}, that are involved in lung cancer have been localized to chromosome bands 3p, 5q, 9p, 11q, and 17 (Slebos and Rodenhuis, 1992; Kern and Filderman, 1993; Pezzella *et al.,* 1993; Prins *et al.,* 1993; Shapiro *et al.,* 1995; Carbone and Kratzke, 1996; Sidransky and Hollstein, 1996), many of the key genes have yet to be identified and characterized. Identification of these genes and an understanding of their role in the initiation and progression

---

[1] Present address: Department of Surgery, University of California, San Francisco, CA 94143.

[2] To whom correspondence should be addressed at National Cancer Institute, Medicine Branch, 9610 Medical Center Drive, Suite 300, Rockville, MD 20850. Telephone: (301) 402-3128. Fax: (301) 402-4422. E-mail: jakowlews@bprb.nci.nih.gov.

of lung cancer may greatly increase our ability to target the genetic lesions that are responsible for malignant transformation and metastasis of this disease.

Several different polypeptide growth factors have been identified in normal lung, including transforming growth factor-β 1 (TGF-β1). TGF-β1 is a multifunctional protein that regulates several diverse biological activities including cell growth, differentiation, adhesion, and migration (reviewed in Derynck and Choy, 1998). In addition, previous studies have shown that TGF-β1 can inhibit anchorage-independent growth of transformed cells (Moses *et al.,* 1985; Roberts *et al.,* 1985), with anchorage-independent growth being a particularly good correlate to tumorigenicity *in vivo* (Shin *et al.,* 1975). TGF-β1 initiates signaling by interacting with its cellular receptors, including the type I (TGF-β RI) and type II (TGF-β RII) receptors, which have been shown to be serine/threonine kinases that are essential components for TGF-β signal transduction (reviewed in Massague', 1998). Ligand binding to constitutively active TGF-β RII results in the recruitment, phosphorylation, and subsequent activation of TGF-β RI in a heteromeric complex. Activated TGF-β RI in the complex in turn propagates the TGF-β signal to downstream effector proteins. Several proteins have been shown to associate with TGF-β receptors, including Smad2 and Smad3. Smad2 and Smad3 are effectors of TGF-β signaling and have been shown to be phosphorylated by activated TGF-β RI, and they subsequently dissociate, form a complex with Smad4/DPC4, and then translocate to the nucleus, where they function as transcriptional activators (Heldin *et al.,* 1997). Smad6 and Smad7 have also been shown to participate in TGF-β signal transduction (Hayashi *et al.,* 1997; Imamura *et al.,* 1997). However, unlike Smad2, Smad3, and Smad 4, Smad6 and Smad7 have been shown to function as negative regulators of TGF-β signaling. In addition to the Smads, other proteins that interact with the TGF-β receptors have been identified. The immunophilin-binding protein FKBP12, a target for the macrolides FK506 and rapamycin, has been shown to interact with the GS domain, or activation domain, of TGF-β RI and to prevent TGF-β signaling in the absence of ligand (Wang *et al.,* 1994; Chen *et al.,* 1997). The α subunit of p21RAS farnesyltransferase, FNTA, has also been shown to interact with the cytoplasmic tail of TGF-β RI (Kawabata *et al.,* 1995; Wang *et al.,* 1996). Two WD-40 domain proteins, the Bα subunit of protein phosphatase 2A (PP2A) (Ventura *et al.,* 1996) and TGF-β RII-interacting protein (TRIP-1) (Chen *et al.,* 1995), associate with TGF-β RI and TGF-β RII, respectively. Recently, human cyclin B2 has been reported to bind directly to TGF-β RII (Liu *et al.,* 1999). Although much of the intracellular signaling mechanism of TGF-β has been elucidated, the whole spectrum of target genes that contribute to the induction and/or maintenance of the specific responses resulting from TGF-β exposure has not been determined. In addition to the important proteins that are required for

transmitting the TGF-β signal from the cytoplasm to the nucleus, there are potentially many other target genes of TGF-β whose protein products may be important in determining the ultimate outcome of TGF-β responsiveness. A number of these TGF-β target genes have been identified and characterized. However, it is likely that there are other TGF-β target genes that have yet to be identified and their functions elucidated in normal and tumor epithelial cells. Thus, identification and characterization of the downstream genes targeted by TGF-β are necessary to understand the nature of TGF-β action in cell processes including proliferation, differentiation, embryogenesis, adhesion, migration, and extracellular matrix formation (Roberts and Sporn, 1990; Roberts *et al.,* 1990; Massague' *et al.,* 1992).

In a previous study, we examined expression of TGF-β ligand and receptor mRNAs and proteins in several non-small-cell lung cancer (NSCLC) and small cell lung cancer (SCLC) cells (Jakowlew *et al.,* 1995). We showed that addition of exogenous TGF-β1 to NSCLC cells inhibited colony formation of some of these cells in soft agarose in a dose-dependent manner. Among the NSCLC cells that we have demonstrated are responsive to TGF-β1 is the NCI-H727 cell line. Anchorage-independent growth of NCI-H727 cells was shown to be inhibited by TGF-β1 (Jakowlew *et al.,* 1995). TGF-β1 mRNA expression was increased after 24 h of treatment of these cells with TGF-β1 (Jakowlew *et al.,* 1995). In the present study, NCI-H727 cells were used as a model system for epithelial cancers to identify potential gene targets involved in TGF-β1-mediated responses using the differential mRNA display method (Liang and Pardee, 1992; Liang *et al.,* 1994). This report describes the identification, cloning, sequencing, and characterization of a novel TGF-β1 target gene in NSCLC cells. This gene, which we named differentially expressed nucleolar TGF-β1 target (DENTT), is differentially induced by TGF-β1 in TGF-β1 responsive NSCLC cells, but not in NSCLC cells that are not responsive to TGF-β1. DENTT mRNA induction by TGF-β1 correlates with induction of TGF-β1 mRNA and with inhibition of anchorage-independent growth in NSCLC cells that are responsive to TGF-β1. DENTT contains a conserved domain that identifies members of the TSPY/TSPY-like/SET/ NAP-1 (TTSN) protein superfamily and signifies DENTT as a new member of this superfamily. DENTT is targeted to the nucleolus minimally by one bipartite nuclear localization signal (NLS) and one monopartite NLS. Thus, nucleolar localization of DENTT may suggest additional roles for the TTSN superfamily.

MATERIALS AND METHODS

Cell culture. Human NSCLC cell lines, including NCI-H157, NCI-H679, NCI-H720, NCI-H727, NCI-H835, NCI-H838, NCI-H1299, NCI-H1435, and NCI-H1734 cells, were cultured in serum-supplemented medium [RPMI 1640 medium (Life Technologies, Rockville, MD) containing 10% heat-inactivated fetal bovine serum

(FBS) (Life Technologies)] at 37°C. Routinely, the cells showed greater than 90% viability, were *Mycoplasma* free, and were used when they were in exponential growth phase. Normal human bronchial epithelial (NHBE) cells obtained from Clonetics (San Diego, CA) were cultured in bronchial epithelial growth medium supplied with the cells. For treatment of cells with TGF-β1, cells were washed with phosphate-buffered saline (PBS) and incubated with ITS medium (RPMI 1640 medium containing 5 μg/ml bovine insulin, 10 μg/ml human transferrin, and 3×10^{-8} M sodium selenite) and 0.1% bovine serum albumin (BSA). Cells were treated with recombinant human TGF-β1 (5 ng/ml) in a vehicle of 4 mM HCl containing 1 mg/ml BSA or vehicle alone. Bovine insulin, human transferrin, sodium selenite, and BSA were purchased from Sigma Chemical Co. (St. Louis, MO). Recombinant human TGF-β1 was obtained from R&D Systems (Minneapolis, MN). Total normal human fetal and adult tissue RNAs were purchased from Clontech (Palo Alto, CA).

Differential mRNA display. Total RNA was isolated by the method of Chirgwin *et al.* (1979) using guanidine isothiocyanate and cesium chloride and subsequently treated with RNase-free DNase (Life Technologies). Purified total cell RNA (0.2 mg) was reverse transcribed in a 20-μl reaction mixture with SuperScript reverse transcriptase (Life Technologies) and oligo(dT) primer 5′-T$_{11}$CA-3′ at 37°C for 60 min. For polymerase chain reaction (PCR) amplification, 2 μl of reverse-transcribed RNA was added to 18 μl of a solution containing the oligo(dT) primer 5′-T$_{11}$CA-3′ and one of 20 different random oligonucleotide primers, including the primer 5′-GAACCT-GAAG-3′. Radioactive α-^{35}S-dATP (Dupont, Boston, MA) was added to the PCR mixture, and the reaction mixture was subjected to 40 cycles of PCR in a Perkin–Elmer-Cetus (Foster City, CA) 9600 Thermal cycler using parameters of 94°C for 30 s, 40°C for 2 min, and 72°C for 30 s according to the RNAimage kit (GenHunter Co., Nashville, TN). Radiolabeled PCR products were analyzed by electrophoresis on 6% polyacrylamide gels. The gels were dried and then exposed to Kodak XAR-5 film (Kodak Co., Rochester, NY).

Reamplification of cDNA fragments. Differentially expressed cDNA fragments were identified, recovered from the gels, and reamplified in a 40-cycle PCR using the same oligonucleotide primer pairs used for differential mRNA display analysis. Reamplified cDNA fragments were separated by electrophoresis on a low-melting agarose gel and extracted using the GeneClean II Kit (Bio 101, Vista, CA). The purified cDNA fragments were then used as templates for random-priming and for TA cloning.

Northern blot analysis. Equal amounts of total RNA (10 μg) were separated by electrophoresis on 1% agarose gels containing 0.66 M formaldehyde, transferred to "Nytran" filters (Schleicher and Schuell, Keene, NH), UV cross-linked, and baked for 3 h. Ethidium bromide (33 μg/ml) was included in both the gels and running buffers to visualize the positions of ribosomal RNAs by UV illumination after electrophoresis. Blots were hybridized with ^{32}P-labeled (3000 Ci/mmol, Dupont) random-primed cDNA probes at 65°C according to Church and Gilbert (1984) and then exposed for various times at -80°C using an intensifying screen. Densitometry of autoradiographs was performed using a scanning laser densitometer (Molecular Dynamics, Sunnyvale, CA).

TA cloning and sequencing analysis. Reamplified cDNA fragments were cloned into the plasmid vector pCRII using the TA cloning kit (Invitrogen, San Diego, CA). Plasmids were purified using the Qiagen plasmid kit according to the manufacturer's directions (Qiagen Inc., Chatsworth, CA). The cDNAs were sequenced with T7 and SP6 oligonucleotide primers using the dye terminator cycle sequencing core kit and an Applied Biosystems automated sequencer (Perkin–Elmer). The nucleotide sequences obtained were compared with known gene sequences by searching the GenBank and EMBL databases with BLAST (National Center for Biotechnology Information, Bethesda, MD).

cDNA library screening. An adult human brain cDNA library was obtained from Clontech and plated out at 1×10^5 colony-forming units per 150-mm plate. Colonies were lifted onto duplicate nitrocel-

lulose filters (Amersham, Boston, MA) and probed as described for Northern blot analysis. Positive colonies were isolated and rescreened after dilution. Secondary and tertiary screening was identical to primary screening.

cDNA probe. Hybridization was performed using the 0.9-kb *Xba*I–*Hin*dIII fragment of rat TGF-β1, plasmid pRTGFβ1 (Qian *et al.,* 1990).

5′ Rapid amplification of cDNA ends (5′ RACE). The 5′-ends of cDNAs were derived using 5′ RACE (Life Technologies) according to the manufacturer's directions. The oligonucleotide primers used for 5′ RACE included GP1 (5′-GCTGGATGATGAGGTCTCTG-3′) for first-strand cDNA synthesis and GP2 (5′-TGAACTTGCGCTTGAGA-3′) for PCR amplification. The PCR products were cloned into the TA cloning vector (Invitrogen), and clones containing inserts were subsequently sequenced.

Generation of enhanced green fluorescent protein fusion constructs. To determine which NLS sequences were required for nuclear localization of DENTT, enhanced green fluorescent protein (EGFP)–fusion constructs were engineered encoding various protein domains of human DENTT. All DENTT cDNAs were cloned into the EGFP carboxyl-terminal protein fusion expression vector pEGFP-C2 (Clontech). EGFP-FL, EGFP-1, EGFP-2, EGFP-3, EGFP-4, EGFP-5, EGFP-6, EGFP-7, EGFP-9, and EGFP-10 were constructed following *Eco*RI–*Bam*HI digestion of PCR products and ligation into similarly digested pEGFP-C2 vector. PCR products were generated using the following oligonucleotide primers:

Construct EGFP-FL: GFP1A, 5′-TCGAATTCATGAGGGGGGT-GGGACTGGG-3′ (nucleotides 25–44); GFP1B, 5′-CGGTGGATC-CGGGAAAACCCTTATCCGGTT-3′ (nucleotides 1917–1936).

Construct EGFP-1: GFP1A, 5′-TCGAATTCATGAGGGGGGGTGG-GACTGGG-3′ (nucleotides 25–44); GFP1C, 5′-CGGTGGATCCGC-CCCTTTCTCTCAGGTAGTA-3′ (nucleotides 1025–1045).

Construct EGFP-2: GFP2A, 5′-GCTTCGAATTCGAGAGAAATGC-CGAGAGGATG-3′ (nucleotides 466–480); GFP2B, 5′-CGGTG-GATCCGCTTCTTTCTCTTTATCCTGGAGCCCCT-3′ (nucleotides 1039–1066).

Construct EGFP-3: GFP3A, 5′-GCTTCGAATTCAAGAAACGTA-AAACCAGGGGC-3′ (nucleotides 1075–1095); GFP4B, 5′-CGGTG-GATCCATTGGCCCAACCGTTTGGGAC-3′ (nucleotides 1885–1905).

Construct EGFP-4: GFP4A, 5′-GCTTCGAATTCTGGGCAGATGT-GAGGTGGTGATC-3′ (nucleotides 1092–1113); GFP1B, 5′-CGGTG-GATCCGGGAAAACCCTTATCCGGTT-3′ (nucleotides 1039–1066).

Construct EGFP-5: GFP1A, 5′-TCGAATTCATGAGGGGGGTGG-GACTGGG-3′ (nucleotides 25–44); GFP2B, 5′-CGGTGGATCCGCT-TCTTTCTCTTTATCCTGGAGCCCCT-3′ (nucleotides 1039–1066).

Construct EGFP-6: GFP1A, 5′-TCGAATTCATGAGGGGGGTGG-GACTGGG-3′ (nucleotides 25–44); GFP4B, 5′-CGGTGGATCCATT-GGCCCAACCGTTTGGGAC-3′ (nucleotides 1885–1905).

Construct EGFP-9: GFP2A, 5′-GCTTCGAATTCGAGAGAAATGC-CGAGAGGATG-3′ (nucleotides 466–480); GFP1B, 5′-CGGTG-GATCCGGGAAAACCCTTATCCGGTT-3′ (nucleotides 1917–1936).

Construct EGFP-10: GFP3A, 5′-GCTTCGAATTCAAGAAACGTA-AAACCAGGGGC-3′ (nucleotides 1075–1095); GFP1B, 5′-CGGTG-GATCCGGGAAAACCCTTATCCGGTT-3′ (nucleotides 1917–1936).

Construct EGFP-7 was generated by PCR amplification of NLS-1 and NLS-4, followed by restriction digestion of NLS-1 and NLS-4 PCR products with *Eco*RI–*Not*I and *Bam*HI–*Not*I (Life Technologies), respectively, and then ligation of the digested fragments. The ligated fragments were cloned into pEGFP-C2 as described above. The PCR oligonucleotide primers used to make EGFP-7 were:

NLS-1: GFP1A, 5′-TCGAATTCATGAGGGGGGTGGGACTGGG-3′ (nucleotides 25–44); GFP3E, 5′- GCGGCCGCGCCCCTTTCTCT-CAGGTAGTA-3′ (nucleotides 1025–1045).

NLS-4: GFP4C, 5′-GCGGCCGCAGGCAGATGTGAGGTGGT-GATC-3′ (nucleotides 1093–1113); GFP1B, 5′-CGGTGGATCCGG-GAAAACCCTTATCCGGTT-3′ (nucleotides 1917–1936).

Construct EGFP-8 was generated by PCR amplification of NLS-1 and NLS-3/NLS-4, followed by restriction digestion of NLS-1 and NLS-3/NLS-4 PCR products with *Eco*RI–*Not*I and *Bam*HI–*Not*I (Life

Technologies), respectively, and then ligation of the digested fragments. The ligated fragments were cloned into pEGFP-C2 as described above. The PCR oligonucleotide primers used to make EGFP-8 included:

NLS-1: GFP1A, 5′-TCGAATTCATGAGGGGGGTGGGACTGGG-3′ (nucleotides 25–44); GFP3E, 5′-GCGGCCGCGCCCCTTTCTCT-CAGGTAGTA-3′ (nucleotides 1025–1045).

NLS-3/NLS-4: GFP3D, 5′-GCGGCCGCAAAGAAACGTAAAAC-CAGGGGC-3′ (nucleotides 1075–1095); GFP1B, 5′-CGGTGGATC-CGGGAAAACCCTTATCCGGTT-3′ (nucleotides 1917–1936).

Transient transfections. A total of 1×10^5 COS-7 cells were seeded in 2-well Lab-Tek chamber slides (Nalge Nunc, Naperville, IL) and grown in DMEM medium (Life Technologies) supplemented with 10% FBS. Twenty-four h later, cells were transfected with EGFP-DENTT vector constructs using Lipofectine according to the manufacturer's directions (Life Technologies). The EGFP expression vector alone and EGFP expression vector containing the previously studied SV40 large T-antigen monopartite NLS sequence, PKKKRKV (Healy *et al.,* 1999), were also transfected into COS-7 cells with Lipofectine and used as negative and positive controls, respectively. Forty-eight h after transfection, cells were washed three times with PBS, fixed with 4% paraformaldehyde in PBS for 30 min at room temperature, washed an additional three times with PBS, stained with DAPI, and mounted with Clear Mount (Biomeda, Foster City, CA). The fixed slides were kept at 4°C until viewed with a Nikon Eclipse E400 microscope with fluorescence and confocal microscopy capabilities (Columbia, MD). Images were captured on film (Universal Imaging Corp., West Chester, PA).

RESULTS

Identification of TGF-β Regulated Genes by Differential Display

We have previously shown that TGF-β1 is able to induce expression of its own mRNA and protein in several NSCLC cell lines, including NCI-H727 cells (Jakowlew *et al.,* 1995). Here, the expression patterns of cDNAs from NCI-H727 cells exposed to TGF-β1 for 24 h and cells exposed to vehicle alone were compared by differential mRNA display analysis to identify new gene targets whose transcription is regulated by TGF-β1. A total of 20 5′-arbitrary decamers were used. Each of the 20 decamers was paired with one of four 3′-degenerate anchored oligo(dT) primers and used to amplify cDNAs synthesized using reverse transcriptase from RNAs extracted from TGF-β1-treated and vehicle-treated NCI-H727 cells with 40 cycles of amplification. All amplifications were performed in duplicate using total RNA extracted from independently treated populations of NCI-H727 cells. The amplified cDNA products were size-fractionated on denaturing urea–polyacrylamide gels, and potential differentially expressed cDNAs were identified by autoradiography. To guard against isolating differentially displayed cDNAs that may be "false positives," only cDNAs whose levels of expression were affected by TGF-β1 in duplicate experiments were selected for further analysis. Representative data are presented in Fig. 1. Five reproducible potential differentially expressed cDNA fragments, designated DD1, DD2, DD3, DD4, and DD5, ranging in size from 100 to 800 bp, were identified by autoradiography. Of the cDNA fragments that were selected for further evaluation, four fragments, includ-
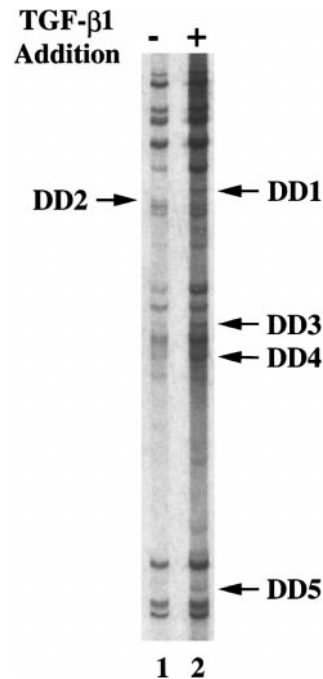
FIG. 1. Differential mRNA display analysis of TGF-β1 regulated genes in NCI-H727 cells. Total RNA was isolated from vehicle-treated (−) (lane **1**) or 5 ng/ml TGF-β1-treated (+) (lane **2**) cultures of NCI-H727 cells and converted to cDNA using reverse transcriptase in the presence of α-^{35}S-dATP for further mRNA differential display amplification. The amplified cDNA fragments were separated by electrophoresis on 6% acrylamide gels, exposed to film, and developed to reveal differential bands as described under Materials and Methods. DD1, DD2, DD3, DD4, and DD5 indicate the position of differentially displayed cDNA bands. The gel shown in this figure is representative of four separate experiments.

ing DD1, DD3, DD4, and DD5, showed an increase in band intensity as a result of TGF-β1 treatment compared with identically sized cDNA fragments from the control vehicle-treated NCI-H727 sample. A single product, DD2, was identified that showed increased band intensity in the vehicle-treated NCI-H727 cDNA sample. The five differentially displayed cDNAs were successfully extracted from acrylamide gels and reamplified.

Northern Blot Analysis of Differentially Displayed cDNA Fragment DD3

Northern blot analysis was used to confirm that the differentially expressed cDNA fragments represent mRNAs whose steady-state levels change following exposure of NCI-H727 cells to TGF-β1. The excised reamplified cDNA fragments were used as probes to hybridize to Northern blots containing total RNA from NCI-H727 cells cultured in the presence of TGF-β1 or vehicle alone for 24 h. Figure 2A shows Northern blot analysis of the DD3 cDNA fragment and hybridization to a transcript of 2.7 kb in NCI-H727 cells. Within 24 h of addition of TGF-β1 to NCI-727 cells, there was at least a 3-fold increase in the level of the transcript of this gene, indicating that it is regulated by TGF-β1. Expression of TGF-β1 mRNA was also examined in
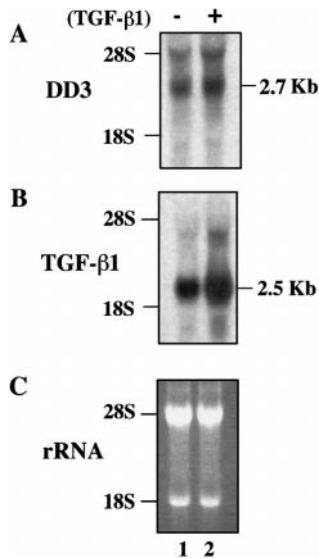
FIG. 2. Northern blot analysis of TGF-β1 regulated mRNAs in NCI-H727 cells. Total RNA (10 μg) was isolated from exponentially proliferating subconfluent NCI-H727 cells cultured for 24 h with: vehicle (lane **1**); 5 ng/ml TGF-β1 (lane **2**), separated by electrophoresis on a 1% agarose gel containing formaldehyde, and transferred to a nylon filter as described under Materials and Methods. Hybridization was performed with (**A**) DD3 cDNA probe; (**B**) TGF-β1 cDNA probe. The blots were exposed for 1 day. (**C**) Ethidium bromide staining pattern of the gel showing 18S and 28S rRNA. The blots shown in this and subsequent figures are representative of three separate experiments.

these cells cultured in the presence or absence of TGF-β1. To examine the expression of TGF-β1 mRNA, the blot that was used to investigate expression of the 2.7-kb TGF-β1 regulated mRNA was dehybridized, exposed to film to ensure complete dehybridization, and then hybridized with a ^{32}P-labeled cDNA probe for

TGF-β1. Hybridization with a TGF-β1 cDNA probe showed an increase in expression of TGF-β1 mRNA of at least 4-fold after exposure of NCI-H727 cells to TGF-β1 (Fig. 2B). As a control, the gel was stained with ethidium bromide and photographed to ensure that equal amounts of RNA had been applied to the gel (Fig. 2C). Northern blot analysis of ^{32}P-labeled DD1, DD2, DD4, and DD5 cDNAs was also performed as for DD3 cDNA with total RNA from TGF-β1-treated and vehicle-treated NCI-727 cells. However, in contrast to DD3, differential expression of the corresponding mRNAs for DD1, DD2, DD4, and DD5 in TGF-β1-treated and vehicle-treated NCI-H727 cells was less than 1.3-fold (data not shown). Due to minimal differential expression of DD1, DD2, DD4, and DD5 mRNAs in response to TGF-β1 by Northern blot hybridization, the identification of the corresponding cDNAs was not pursued, and efforts were made to identify DD3 cDNA.

To determine whether expression of DD3 mRNA is affected by TGF-β1 in other lung cancer and normal lung cells, the expression of DD3 mRNA was examined in additional NSCLC cell lines and NHBE cells. Figure 3A shows that the 2.7-kb DD3 transcript was detectable in NCI-H157 squamous cell carcinoma, NCI-H838 adenocarcinoma, NCI-H1299 large cell carcinoma, and NHBE cells by Northern blot analysis with a ^{32}P-labeled DD3 cDNA probe. After addition of exogenous TGF-β1 to these cells for 24 h, Fig. 3A also shows there was a 1.5- and 4-fold increase in expression of DD3 mRNA in NCI-H157 and NCI-H1299 cells, respectively. At the same time, there was no change in DD3 mRNA in NCI-H838 or NHBE cells after addition of TGF-β1 to these cells (Fig. 3A). Hybridization of DD3 cDNA to RNA from four additional NSCLC carcinoid
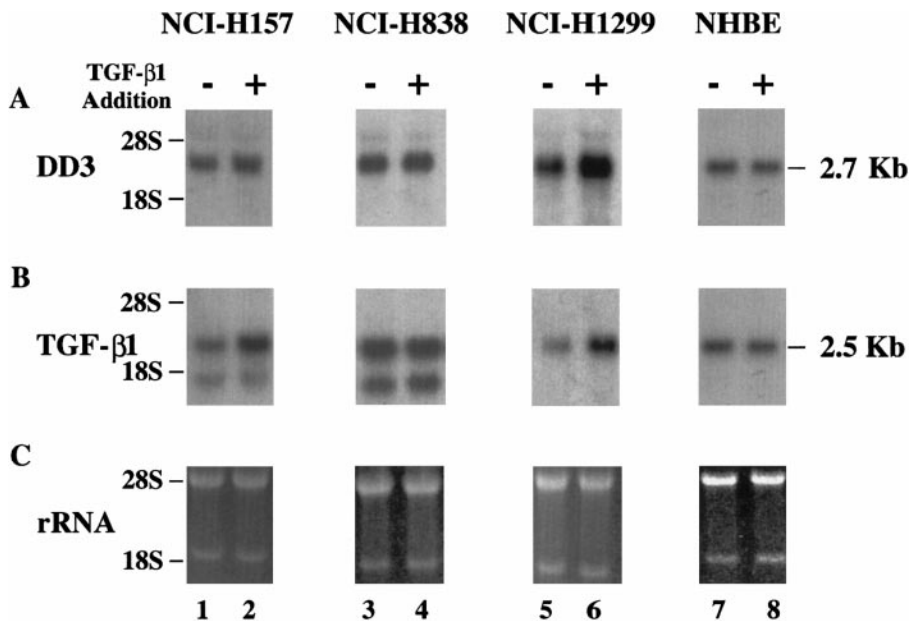
FIG. 3. Northern blot analysis of DD3 and TGF-β1 mRNAs in NSCLC and NHBE cells. Total RNA (10 μg) was isolated from exponentially proliferating subconfluent NCI-H157, NCI-H838, NCI-H1299, and NHBE cells cultured for 24 h with: vehicle (lanes **1, 3, 5,** and **7**); 5 ng/ml TGF-β1 (lanes **2, 4, 6,** and **8**), and analyzed as before with (**A**) DD3 cDNA probe; (**B**) TGF-β1 cDNA probe. The blots were exposed for 1 day. (**C**) Ethidium bromide staining pattern of the gel showing 18S and 28S rRNA.
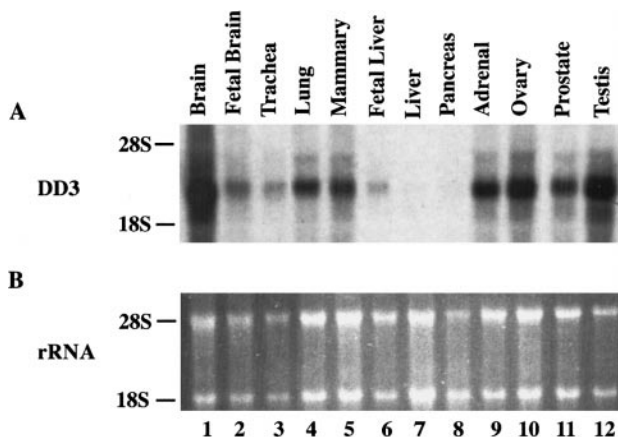
FIG. 4. Northern blot analysis of DD3 mRNA in normal human tissues. Total RNA (10 μg) isolated from nomal human tissues, including brain (lane **1**); fetal brain (lane **2**); trachea (lane **3**); lung (lane **4**); mammary gland (lane **5**); fetal liver (lane **6**); liver (lane **7**); pancreas (lane **8**); adrenal gland (lane **9**); ovary (lane **10**); prostate (lane **11**); testis (lane **12**), was separated by gel electrophoresis, transferred to a nylon filter, and analyzed as before with (**A**) DD3 cDNA probe. The blot was exposed for 2 days. (**B**) Ethidium bromide staining pattern of the gel showing 18S and 28S rRNA.

cell lines cultured in the presence of TGF-β1, including NCI-H679, NCI-H720, NCI-H835, NCI-H1435, and NCI-H1734 cells, showed no more than a 1.2-fold increase in DD3 mRNA (data not shown). Dehybridization of these blots and subsequent hybridization with a TGF-β1 cDNA probe showed a 4- to 6-fold increase in TGF-β1 mRNA in NCI-H157 and NCI-H1299 cells upon addition of TGF-β1 to these cells (Fig. 3B). No change in TGF-β1 mRNA expression was detected in NCI-H838 cells after addition of exogenous TGF-β1, as we have previously reported (Jakowlew *et al.,* 1995).

Following Northern blot hybridization analysis, the DD3 TGF-β1 regulated cDNA fragment was subcloned into plasmid DNA. The insert from this plasmid DNA was also shown to hybridize to the same size mRNA and to exhibit differential expression in TGF-β1-treated and vehicle-treated NCI-H727 cells (data not shown). It was determined that this plasmid DNA fragment had an insert of 496 bp, and DNA sequence analysis confirmed that it contained both 5′- and 3′-oligonucleotide primer sequences used for amplification (data not shown). After DNA sequence homology searches in the GenBank and EMBL databases, the sequence of DD3 cDNA showed no significant matches with any known gene sequence. Thus, DD3 may be a novel target gene of TGF-β1.

Expression of DD3 mRNA in Human Tissues

Expression of DD3 mRNA was examined in various human tissues using Northern blot analysis. Figure 4 shows hybridization of DD3 cDNA to total RNA from 12 normal human tissues. The highest levels of expression of DD3 mRNA occurred in brain and testis. Compared to adult brain and testis, moderate levels of DD3 mRNA expression were detected in lung, mammary gland, adrenal gland, ovary, and prostate, while only low levels of this mRNA were detected in adult trachea, fetal brain, and fetal liver. In addition, very low, but detectable levels of DD3 mRNA were observed in adult liver and pancreas after prolonged exposure (data not shown).

Cloning and Sequence Analysis of Full-length DD3 cDNA

A normal, adult, human brain cDNA library was screened with the 496-bp DD3 cDNA fragment, and several positive clones were identified. The longest clones were approximately 1.4 kb in length. The DNA from these clones was sequenced, and sequence homology searches of databases indicated that the 1.4-kb DD3 cDNA, like the 496-bp DD3 cDNA, had no significant matches to any known gene sequence. 5′ RACE and genome walking were performed to obtain the remaining 5′-portion of DD3 cDNA. The nucleotide sequence of full-length DD3 mRNA, consisting of 2569 bp, is shown in Fig. 5, together with the deduced amino acid sequence. This is in agreement with the estimated 2.7-kb size of DD3 mRNA by Northern blot analysis shown in Fig. 2A. The sequence of full-length DD3 was determined to have no significant matches with any known gene sequence. Thus, DD3 is a novel TGF-β1 target gene that we have named DENTT. DENTT cDNA contains a 5′-UTR consisting of 58 nucleotides. In addition, DENTT cDNA contains an 1899-bp open reading frame (ORF) that encodes a predicted 633-amino-acid protein of 72,800 Da. The amino acid sequence shown in Fig. 5 represents the longest ORF with the ATG triplet at nucleotide 59 being the translational initiation site. The translational initiation site was tentatively assigned to the ATG triplet at nucleotide 59, rather than to the ATG triplet farther downstream at nucleotide 425 for the following reasons. According to the translational "scanning model" (Kozak, 1981a), eukaryotic ribosomes bind to the 5′-terminus of mRNA and migrate along the mRNA sequence until they encounter the first AUG triplet, which, by virtue of its location, is the initiation codon. An extended version of the scanning model was proposed in which the nucleotides flanking the AUG initiation codon play an important role in the recognition by eukaryotic ribosomes (Kozak, 1981b, 1982). According to this version, the most favorable sequence for initiation is A/GNNAUGG. Although the ATG triplet at nucleotide 425 corresponds to the most favorable sequence for initiation, the upstream ATG triplet at nucleotide 59 has a more suitable location for translational initiation according to the scanning model. We have chosen the ATG triplet at nucleotide 59 as the translational initiation triplet that results in the longest ORF. DNA sequence analysis also showed that DENTT contains a 14-residue poly(A) sequence at its 3′-end indicating the 3′-poly(A) tail of DENTT mRNA. Interestingly, the 496-bp DENTT cDNA fragment that
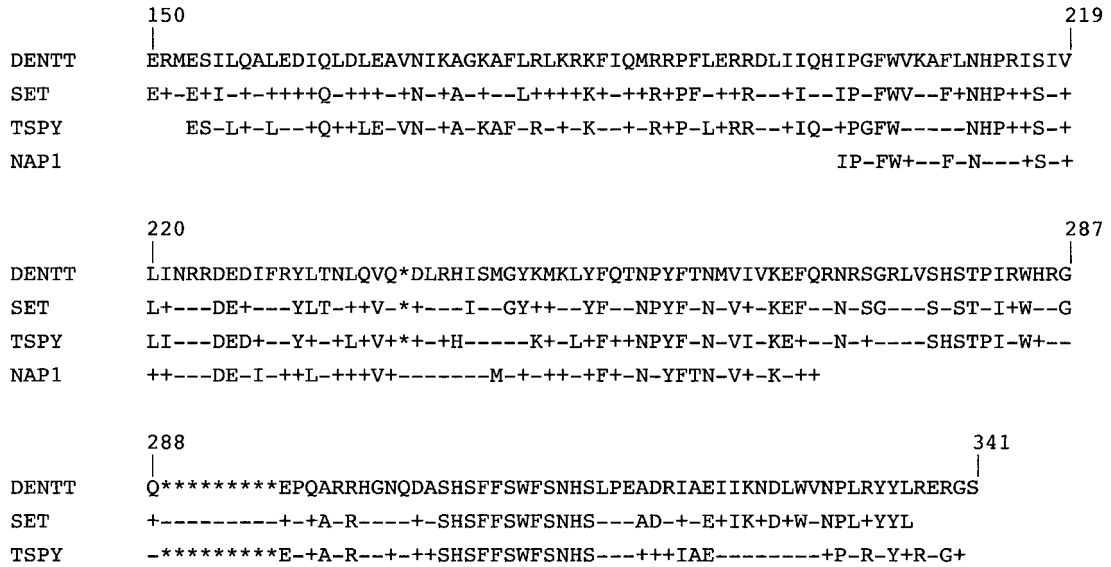
```
  1    ACCCCAGCAG     CGCCCGAGGC     TCCAGGAGGA     AACGGGAGGCG    GCACAGGTGC     TGGCCGAT
 59    ATG AGG GGG    GTG GGA CTG    GGC CCC GCG    CTG CCC CCG    CCG CCT CCC    TAT GTC ATT CTC
       M   R   G     V   G   L     G   P   A     L   P   P     P   P   P     Y   V   I   L      19
116    GAG GAG GGG    GGG ATC CGC    GCA TAC TTC    ACG CTC GGT    GCT GAG TGT    CCC GGC TGG GAT
       E   E   G     G   I   R     A   Y   F     T   L   G     A   E   C     P   G   W   D      38
173    TCT ACC ATC    GAG TCG GGG    TAT GGG GAG    GCG CCC CCG    CCC ACGGAG     AGC CTG GAA GCA
       S   T   I     E   S   G     Y   G   E     A   P   P     P   T   E     S   L   E   A      57
230    CTC CCC ACT    CCT GGC GCC    TCG GGG GGG    AGC CTG GAA    ATC GAT TTT    CAG GTT GTA CAG
       L   P   T     P   E   A     S   G   G     S   L   E     I   D   F     Q   V   V   Q      76
287    TCG AGC AGT    TTT GGT GGT    GGA GAG GGG    GCC CTA GAA    ACC TGT AGC    GCA GTG GGG TGG GCG
       S   S   S     F   G   G     G   E   G     A   L   E     T   C   S     A   V   G   W   A   95
344    CCC CAG AGG    TTA GTT GAC    CCG AAG AGC    AAG GAA GAA    GAG GCG ATC    ATC ATA GTG GAG GAT
       P   Q   R     L   V   D     P   K   S     K   E   E     E   A   I     I   I   V   E   D   114
401    GAG GAT GAG    GAT GAG CGG    GAG AGT ATG    AGG AGC AGC    AGG AGG CGG    CGG CGG CGG CGG
       E   D   E     D   E   R     E   S   M     R   S   S     R   R   R     R   R   R   R      133
458    AGG AGG AAG    CAG AGG AAG    GTG AAG AGG    GAA AGC AGA    GAG AGA AAT    GCC GAG AGG ATG
       R   R   K     Q   R   K     *V  *K  *R    *E  *S  *R    *E  *R  *N    *A  *E  *R  *M     152
515    GAG AGC ATC    CTG CAG GCA    CTG GAT ATT    CAG CTG GAT    CTG GAG GCA    GTG AAC ATC
       *E  *S  *I    *L  *Q  *A    *I  *E  *D    *I  *Q  *I    *D  *I  *E    *A  *V  *N  *I     171
572    AAG GCA GGC    AAA GCC TTC    CTG CGT CTC    AAG CGC AAG    TTC ATC CAG    ATG CGA AGA CCC
       *K  *A  *G    *K  *A  *F    L   R   L     K   R   K     F   I   Q     M   R   R   P      190
629    TTC CTG GAG    CGC AGA GAC    CTC ATC ATC    CAG CAT ATC    CCA GGC TTC    TGG GTC AAA GCA
       F   L   E     R   R   D     L   I   I     Q   H   I     P   G   F     W   V   K   A      209
686    TTC CTC AAC    CAC CCC AGA    ATT TCA ATT    TTG ATC AAC    CGA CGT GAT    GAA GAC ATT TTC
       F   L   N     H   P   R     I   S   I     L   I   N     R   R   D     E   D   I   F      228
743    CGC TAC TTG    ACC AAT CTG    CAG GTA CAG    GAT CTC AGA    CAT ATC TCC    ATG GGC TAC AAA
       R   Y   L     T   N   L     Q   V   Q     D   L   R     H   I   S     M   G   Y   K      247
800    ATG AAG CTG    TAC TTC CAG    ACT AAC CCC    TAC TTC ACA    AAC ATG GTG    ATT GTC AAG GAG
       M   K   L     Y   F   Q     T   N   P     Y   F   T     N   M   V     I   V   K   E      266
857    TTC CAG CGC    AAC CGC TCA    GGC CGG CTG    GTG TCT CAC    TCA ACC CCA    ATC CGC TGG CAC
       F   Q   R     N   R   S     G   R   L     V   S   H     S   T   P     I   R   W   H      285
914    CGG CAG GAA    GAA CCC CAG    GCC CGT CGT    CAC GGG AAC    CAG GAT GCG    AGC CAC AGC TTT
       R   Q   E     E   P   Q     A   R   R     H   G   N     Q   D   A     S   H   S   F      304
971    TTC AGC TGG    TTC TCA AAC    CAT AGC CTC    CCA GAG GCT    GAC AGG ATT    GCT GAG ATT ATC
       F   S   W     F   S   N     H   S   L     P   E   A     D   R   I     A   E   I   I      323
1028   AAG AAT GAT    CTG TGG GTT    AAC CCT CTA    CGC TAC TAC    CTG AGA GAA    AGG GGC TCC AGG
       K   N   D     L   W   V     N   P   L     R   Y   Y     L   R   E     R   G   S   R      342
1085   ATA AAG AGA    AAG AAG CAA    GAA ATG AAG    AAA CGT AAA    ACC AGG GGC    AGA TGT GAG GTG
       I   K   R     K   K   Q     E   M   K     K   R   K     T   R   G     R   C   E   V      361
1142   GTG ATC ATG    GAA GAC GCC    CCT GAC TAT    TAT GCA GTG    GAA GAC ATT    TTC AGC GAG ATC
       V   I   M     E   D   A     P   D   Y     Y   A   V     E   D   I     F   S   E   I      380
1199   TCA AAC ATT    GAT GAG ACA    ATT CAT GAC    ATC AAG ATC    TCT GAC TTC    ATG GAG ACC ACC
       S   N   I     D   E   T     I   H   D     I   K   I     S   D   F     M   E   T   T      399
1256   GAC TAC TTC    GAG ACC ACT    GAC AAT GAG    ATA ACT GAC    ATC AAT GAG    AAC ATC TGC GAC
       D   Y   F     E   T   T     D   N   E     I   T   D     I   N   E     N   I   C   D      418
1313   AGC GAG AAT    CCT GAC CAC    AAT GAG GTC    CCC AAC AAC    GAG ACC ACT    GAT AAC AAC GAG
       S   E   N     P   D   H     N   E   V     P   N   N     E   T   T     D   N   N   E      437
1370   AGT GCT GAT    GAC CAC GAA    ACC ACTGAC    AAC AAT GAG    AGT GCA GAT    GAC AAC AAC GAG
       S   A   D     D   H   E     T   T   D     N   N   E     S   A   D     D   N   N   E      456
1427   AAT CCT GAA    GAC AAT AAC    AAG AAC ACT    GAT GAC AAC    GAA GAG AAC    CCT AAC AAC AAC
       N   P   E     D   N   N     K   N   T     D   D   N     E   E   N     P   N   N   N      475
1484   GAG AAC ACT    TAC GGC AAC    AAC TTC TTC    AAA GGT GGC    TTC TGG GGC    AGC CAT GGC AAC
       E   N   T     Y   G   N     N   F   F     K   G   G     F   W   G     S   H   G   N      494
1541   AAC CAG GAC    AGC AGC GAC    AGT GAC AAT    GAA GCA GTT    GAG GCC AGT    GAT GAT GAA GAT
       N   Q   D     S   S   D     S   D   N     E   A   V     E   A   S     D   D   E   D      513
1598   AAT GAT GGC    AAC GAA GGT    GAC AAT GAG    GGC AGT GAT    GAT GAT GAC    AAT GAA GGT GAC
       N   D   G     N   E   G     D   N   E     G   S   D     D   D   D     N   E   G   D      532
1655   AAT GAA GGC    AGC GAT GAT    GAC GAC AGA    GAC ATT GAG    TAC TAT GAG    AAA GTT ATT GAA
       N   E   G     S   D   *D    *D  *D  *R    *D  *I  *E    *Y  *Y  *E    *K  *V  *I  *E     551
1712   GAC TTT GAC    AAG GAT CAG    GCT GAC TAC    GAG GAC GTG    ATA GAG ATC    ATC TCA GAC GAA
       *D  *F  *D    *K  *D  *Q    *A  *D  *Y    *E  *D  *V    *I  *E  *I    *I  S   D   E      570
1769   TCA GTG GAA    GAA GAG GGC    ATT GAG GAG    GGC ATC GAA    GAT GAG GAC    ATC TAT GAG
       S   V   E     E   E   G     I   E   E     G   I   Q     Q   D   E     D   I   Y   E      589
1826   GAA GGA AAC    TAT GAG GAG    GAA GGA AGT    GAA GAT GTC    TGG GAA GAA    GGG GAA GAT TCG
       E   G   N     Y   E   E     E   G   S     E   D   V     W   E   E     G   E   D   S      608
1883   GAC GAC TCT    GAC CTA GAG    GAT GTG CTT    CAG GTC CCA    AAC GGT TGG    GCC AAT CCG GGG
       D   D   S     D   L   E     D   V   L     Q   V   P     N   G   W     A   N   P   G      627
1940   AAG AGG GGG    AAA ACC GGA    TAA
       K   R   G     K   T   G     *                                                            633
1961   GGGTTTTCCC     CTTTTGGGGA     TCACCTCTCT     GTATCCCCCA     CCCACTATCC     CATTTGCCCT     CCTCCTCAGC
2031   TAGGGCCACG     CGGCCCCACA     TTGCACTTCT     GGGGGGTGAC     CGACTTCGTA     CACGGGTTTA     AAGTTTATTT
2101   TTATGGTTTA     GTCATTGCAA     ATTCTTATTT     TGGGGGGAAG     GAAAAGGGGC     TAGTCCCTTC     TTTTGGCCTC
2171   CGCCCCGCAA     GCTTCTGTGT     GCTGCTAACT     GTATTTATTG     TGATGCCTTG     GTCAGGGCCC     CTCTCACCCAC
2241   TTCTCCCAGT     CAGTTGTGGC     CCCAGCCCCT     CTCCCTGTGC     TGTGTGGAGT     GGACACCCTG     ACCCCCGAAG
2311   CGGGAGGGCC     GCTGTGGCCT     TCGTCACAGC     CGCGCAGTGC     CCATGGAGGC     GCAAGCTAGC     CACCTTCCTC
2381   TCCCAAGTTC     TTTCTCCATC     CCTCTCCTCT     TCCCGCGCGC     CGCTAGCCCG     CCTCGGTGTC     TATGCAAGGC
2451   CCTTCGCCAT     TGCGGTATTC     TTTGCGGTAT     TCTTGTCCCC     GTCCCCCAGA     AGGCTCGCCT     CTCCCCGTGG
2521   ACCCTGTTAA     TCCCAATAAA____ATTCTGAGCA     AGTTCAAAAA     AAAAAAAAA
```

FIG. 5. Nucleotide sequence and deduced amino acid sequence of differentially expressed nucleolar TGF-β1 target (DENTT). Numbers to the left correspond to the nucleotide sequence with nucleotide number 1 as the first T after the oligonucleotide primer. Numbers to the right correspond to the single-letter amino acid sequence with methionine number 1 as the first in-frame amino acid. The amino acids of four potential nuclear localization signals (NLS) are in boldface type. Two potential coiled-coil regions are designated by boldface asterisks next to each amino acid. The amino acid region of similarity to the TSPY/SET/NAP-1 protein superfamily is double underlined. The nucleotides of the 496-bp DD3 cDNA sequence are underlined. The TAA translational termination codon is indicated by an asterisk. The poly(A) addition site is dash underlined.

was recovered by differential mRNA display was not found adjacent to the poly(A) tail sequence of the 1.4-kb cDNA clones, but instead was located 616 bp upstream of the poly(A) tail as shown in Fig. 5. The 3′-UTR region of DENTT consists of 595 bp between the trans-

lation termination signal and the poly(A) tail sequence. It has been shown that the hexanucleotide AAUAAA found 15–25 nucleotides upstream from the polyadenylation site in most eykaryotic mRNAs serves as part of the signal for polyadenylation (Proudfoot and

```
              150                                                                    219
              |                                                                      |
DENTT         ERMESILQALEDIQLDLEAVNIKAGKAFLRLKRKFIQMRRPFLERRDLIIQHIPGFWVKAFLNHPRISIV
SET           E+-E+I-+-++++Q-+++-+N-+A-+--L++++K+-++R+PF-++R--+I--IP-FWV--F+NHP++S-+
TSPY              ES-L+-L--+Q++LE-VN-+A-KAF-R-+-K--+-R+P-L+RR--+IQ-+PGFW-----NHP++S-+
NAP1                                                           IP-FW+--F-N---+S-+


              220                                                                    287
              |                                                                      |
DENTT         LINRRDEDIFRYLTNLQVQ*DLRHISMGYKMKLYFQTNPYFTNMVIVKEFQRNRSGRLVSHSTPIRWHRG
SET           L+---DE+---YLT-++V-*+---I--GY++--YF--NPYF-N-V+-KEF--N-SG---S-ST-I+W--G
TSPY          LI---DED+--Y+-+L+V+*+-+H-----K+-L+F++NPYF-N-VI-KE+--N-+----SHSTPI-W+--
NAP1          ++---DE-I-++L-+++V+-------M-+-++-+F+-N-YFTN-V+-K-++


              288                                                                    341
              |                                                                      |
DENTT         Q*********EPQARRHGNQDASHSFFSWFSNHSLPEADRIAEIIKNDLWVNPLRYYLRERGS
SET           +---------+-+A-R----+-SHSFFSWFSNHS---AD-+-E+IK+D+W-NPL+YYL
TSPY          -*********E-+A-R--+-++SHSFFSWFSNHS---+++IAE--------+P-R-Y+R-G+
```

FIG. 6. Alignment of the predicted DENTT amino acid sequence with that of human SET, TSPY, and NAP-1. The alignment and region of similarity were identified using the BLAST program. Numbers above the DENTT sequence correspond to the amino acid sequence. Identity is indicated using the single-letter amino acid code. Conservative amino acid chages are indicated by a plus sign. Nonconservative amino acid changes are indicated by dashes. Asterisks indicate gaps that were introduced to align regions of similarity between sequences.

Brownlee 1976; Fitzgerald and Shenk, 1981; Montell *et al.*, 1983). In DENTT, this polyadenylation signal is found 15 nucleotides upstream from the poly(A) tail sequence.

Computer analysis software programs, including MOTIFS and PSORT, were used to analyze the deduced DENTT amino acid sequence. According to PSORT, the DENTT ORF has four putative NLSs including RRRRRRRRRKQRKVKRE, located at amino acid residues 127–143, KRKK, located at amino acids 344–347, KKRK, located at amino acids 351–354, and PGKRGKT, located at amino acids 628–633. The first NLS (NLS-1) conforms to the consensus sequence for a bipartite NLS (Dingwall and Laskey, 1991), and the other three NLSs (NLS-2, NLS-3, and NLS-4) resemble the monopartite NLS classes (Kalderon *et al.*, 1984). PSORT calculation gives a 78% probability that DENTT is localized to the nucleus. In addition to the NLS regions, two potential coiled coil regions are located at amino acid residues 140–177 and 538–567 (Fig. 5). The programs also predict that DENTT does not contain an N-terminal signal sequence for transfer into the endoplasmic reticulum or a hydrophobic region that is characteristic of transmembrane proteins.

A database homology search for the DENTT amino acid sequence was performed using the National Center for Biotechnology Information BLAST Network Service. This search identified a conserved 191-amino-acid domain in DENTT located between amino acid residues 150 and 341 that showed significant identity to, and defines, the testis-specific protein, Y-encoded/testis-specific protein, Y-encoded-like/SET/nucleosome assembly protein-1 (TSPY/TSPY-like/SET/NAP-1, or TTSN) protein superfamily (Tyler-Smith *et al.*, 1988; Ishimi *et al.*, 1984; Weissenbach *et al.*, 1989; Ishimi and Kikuchi, 1991; Von Lindern *et al.*, 1992; Adachi *et al.*, 1994; Vogel *et al.*, 1998) (Fig. 6). An alignment of the predicted DENTT amino acid sequence with human SET, TSPY, and NAP-1 was performed. Figure 6 shows that this alignment demonstrated 34, 40, and 30% amino acid sequence identity of DENTT with SET (GenBank Accession No. AAC50460), TSPY (GenBank Accession No. AAB51693), and NAP-1 (GenBank Accession No. AAA34811), respectively. When the alignment is performed to allow conservative amino acid changes, the amino acid alignment shows 64, 61, and 57% sequence identity of DENTT with SET, TSPY, and NAP-1, respectively. Thus, DENTT may be a new member of the TTSN protein superfamily.

Subcellular Localization of DENTT

Because members of the TTSN family are localized to the nucleus, and DENTT has four potential NLSs and is predicted by PSORT to localize to the nucleus, we sought to determine whether DENTT was localized to the nucleus by enhanced green fluorescence. Full-length DENTT encoding amino acids 1–633 was expressed as a carboxyl-terminal fusion protein of EGFP to generate the construct EGFP-FL by incorporating DENTT cDNA into pEGFP-C2, an expression vector containing the gene encoding EGFP. Sequence analysis indicated that this construct containing the four potential NLSs was in-frame with EGFP (data not shown). Because DENTT was identified as a target gene of TGF-β1 in NSCLC cells, we initially preferred to analyze DENTT localization in NCI-H727 cells. However, the low transfection efficiency in these cells precluded their use when large numbers of transfectants were required. The higher transfection efficiency of COS-7 cells permitted these analyses. In addition, COS-7 cells have more distinct nuclei that are easily
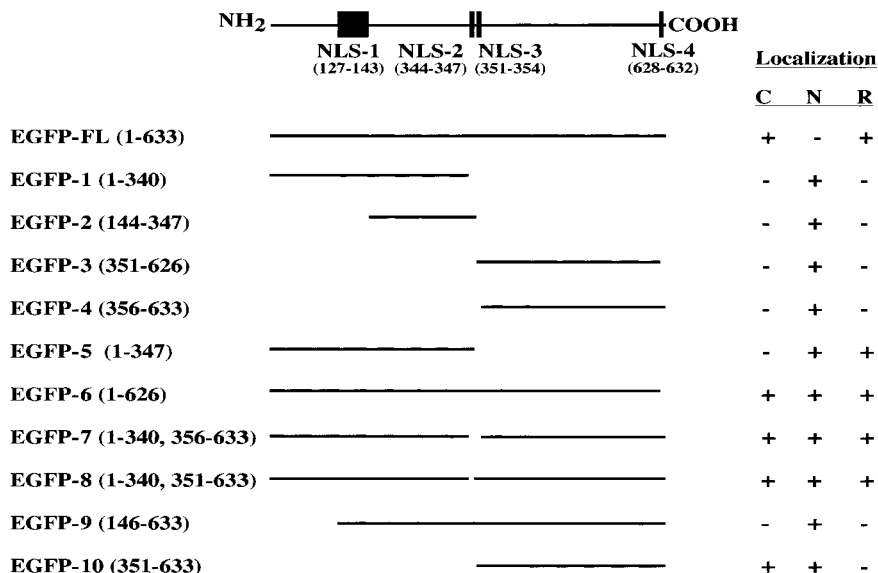
NH₂ — [NLS-1 (127-143)] NLS-2 (344-347) NLS-3 (351-354) NLS-4 (628-632) — COOH

Construct	Localization		
	C	N	R
EGFP-FL (1-633)	+	-	+
EGFP-1 (1-340)	-	+	-
EGFP-2 (144-347)	-	+	-
EGFP-3 (351-626)	-	+	-
EGFP-4 (356-633)	-	+	-
EGFP-5 (1-347)	-	+	+
EGFP-6 (1-626)	+	+	+
EGFP-7 (1-340, 356-633)	+	+	+
EGFP-8 (1-340, 351-633)	+	+	+
EGFP-9 (146-633)	-	+	-
EGFP-10 (351-633)	+	+	-

FIG. 7. EGFP–DENTT full-length and deletion fusion constructs and their subcellular localization in COS-7 cells. Shown is a schematic of the amino acid sequence of DENTT indicating four potential nuclear localization signals (NLS). The full-length and deletion constructs are identified on the left. The subcellular localization of DENTT is indicated on the right. C denotes predominately cytoplasmic staining. N denotes predominately nuclear staining. R denotes predominately nucleolar staining.

identified from the cytoplasm than NCI-H727 cells. After transfection of EGFP-FL into COS-7 cells, the subcellular localization of the fusion protein was determined by fluorescence microscopy. Fluorescence of transfected EGFP-FL was observed in the cytoplasm and nucleolus and was distinctly excluded from the nucleus in 95% of the transfected cells showing green fluorescence (Fig. 8A). The corresponding DAPI stained image is shown in Fig. 8B.

Intrigued by the nucleolar localization of DENTT, the minimum number of DENTT NLS domains that are capable of mediating its localization to the nucleolus was determined. For this, a series of deletion mutants was generated, as diagrammed in Fig. 7. All constructs used in this study were sequenced to verify that they were in-frame with EGFP (data not shown). The DENTT mutant proteins were expressed as carboxyl-terminal fusions of EGFP, and after transient transfection expression in COS-7 cells, the subcellular localization of each fusion protein was determined by fluorescence microscopy as for EGFP-FL. Representative fluorescence micrographs are shown in Fig. 8, and the distinct subcellular localizations were seen in 90–95% of the transfected cells.

The DENTT NLS domains were examined to determine their effect on nucleolar localization. Analysis of the predicted amino acid sequence of DENTT revealed an excellent candidate bipartite NLS at amino acids 127 to 143 (NLS-1, Fig. 5). This region contains 4 basic amino acids, an 8-residue spacer region, and a basic cluster in which 4 of the 5 amino acids are basic. To determine whether the amino terminus of DENTT by itself could direct nuclear localization, the region of DENTT containing only amino acids 1–340, was fused to EGFP to generate the construct EGFP-1 (Fig. 7). In COS-7 cells transfected with EGFP-1, the majority of fluorescence was localized to the nucleus, although some fluorescence was also observed in the cytoplasm (Fig. 8C). To determine whether the second potential NLS (NLS-2) in DENTT, consisting of three lysine residues and one arginine residue at amino acids 344–347, could affect subcellular localization of DENTT, the region of DENTT containing amino acids 144–347 was fused to EGFP to generate the construct EGFP-2 (Fig. 7). When COS-7 cells were transfected with this construct, fluorescence was detected in the nucleus (Fig. 8E). However, unlike the uniform pattern of fluorescence that was observed using EGFP-1, the nuclear fluorescence pattern of EGFP-2 was speckled. Transfection of COS-7 cells with a construct containing only the third NLS (NLS-3), consisting of three lysine residues and one arginine residue at amino acids 351–354, fused to EGFP designated EGFP-3 (Fig. 7), also showed fluorescence in the nucleus with a speckled pattern similar to that of EGFP-2 (Fig. 8G). To determine whether fluorescence from EGFP-1, EGFP-2, and EGFP-3 localized to the nucleolus, confocal microscopy was used. Figures 9A and 9B show that fluorescence from EGFP-1 and EGFP-2 localized only to the nucleus. Confocal microscopy showed a similar nuclear localization pattern for EGFP-3 (data not shown). Transfection with construct EGFP-4 containing only the fourth NLS (NLS-4) at amino acids 628–632, consisting of two lysine residues, one arginine residue, two glycine residues, and one threonine residue, showed uniform fluorescence in the nucleus, and, interestingly, it was excluded from the nucleolus (Fig. 8H).

Since no DENTT NLS by itself showed the same nucleolar localization pattern that full-length DENTT did, various combinations of the four DENTT NLSs were generated to determine the minimum number of NLSs needed for nucleolar localization of DENTT.
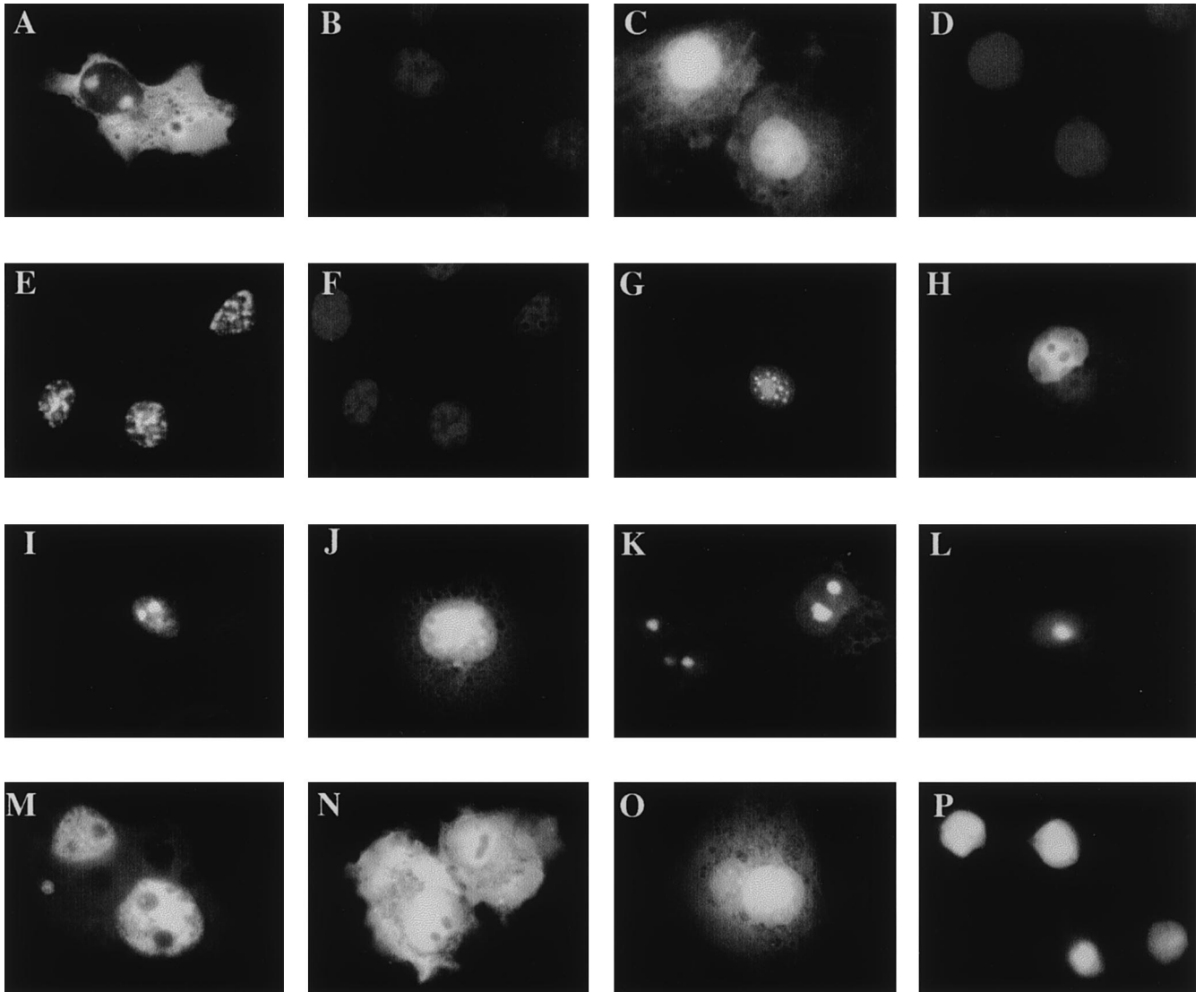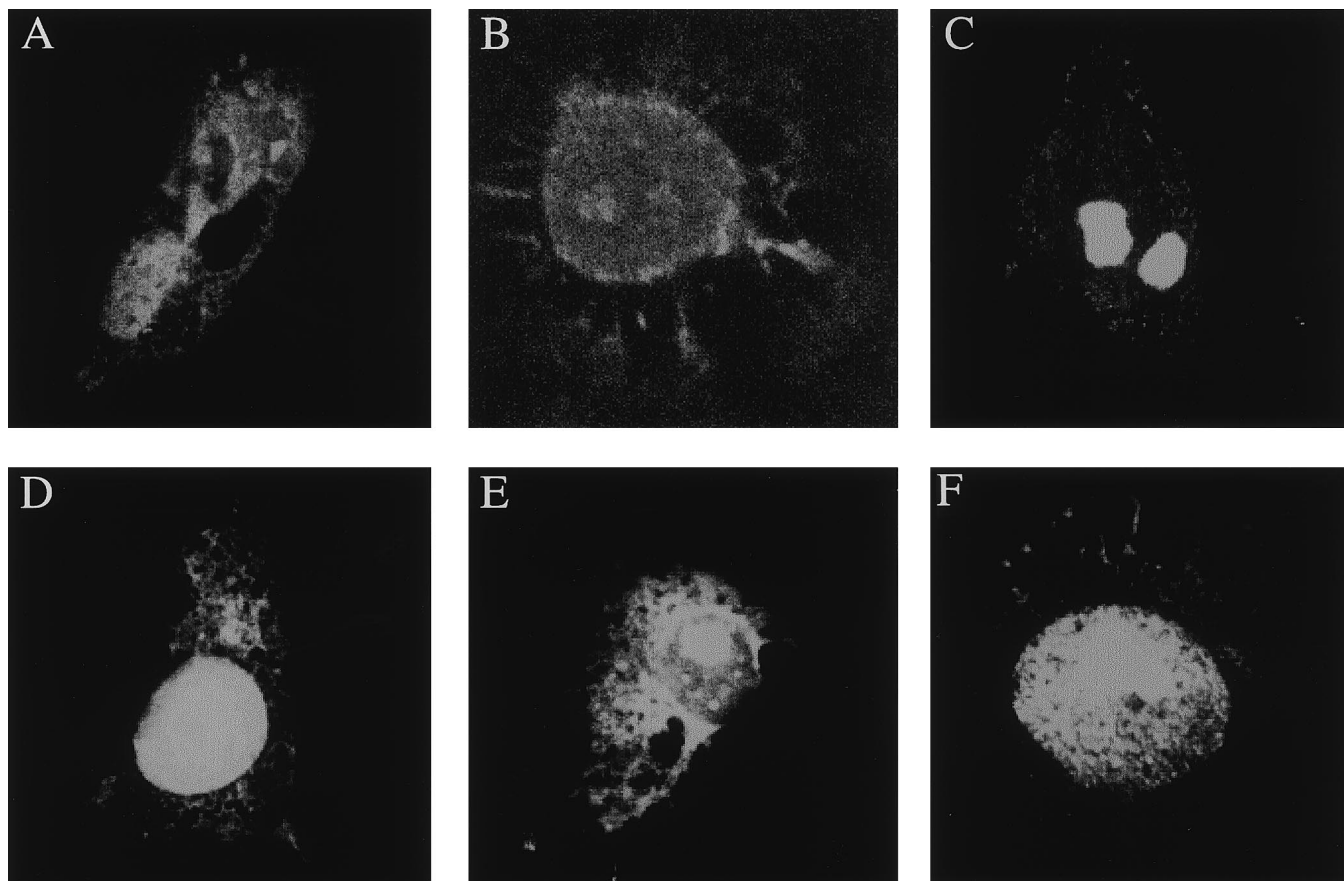
FIG. 8. Subcellular localization of fusion proteins containing EGFP linked to portions of the DENTT protein using fluorescence microscopy. COS-7 cells were transfected with EGFP fused to (**A**) DENTT(aa 1–633) = EGFP-FL; (**C**) DENTT (aa 1–340) = EGFP-1; (**E**) DENTT (aa 144–347) = EGFP-2; (**G**) DENTT (aa 351–626) = EGFP-3; (**H**) DENTT (aa 356–633) = EGFP-4; (**I**) DENTT (aa 1–347) = EGFP-5; (**J**) DENTT (aa 1–626) = EGFP-6; (**K**) DENTT (aa 1–340, 356–633) = EGFP-7; (**L**) DENTT (aa 1–340, 351–633) = EGFP-8; (**M**) DENTT (aa 146–633) = EGFP-9; (**N**) DENTT (aa 351–633) = EGFP-10; (**O**) EGFP-C2 vector; (**P**) GFP/SV40-NLS plasmid. COS-7 cells that were transiently transfected with EGFP fused to DENTT were also stained with DAPI. (**B, D,** and **F**) DAPI staining of EGFP-FL, EGFP-1, and EGFP-2, respectively. Representative cells from transient transfections were photographed using fluorescence microscopy, and greater than 95% of transfected cells showed representative subcellular localization. Results are representative of four independent experiments.

Generation of construct EGFP-5, which contains NLS-1 and NLS-2, and transfection showed localization of fluorescence primarily in the nucleolus, although some fluorescence was also apparent in the nucleus (Fig. 8I). Confocal localization of fluorescence to the nucleus and nucleolus from EGFP-5 was also shown by confocal microscopy (Fig. 9C). Transfection of EGFP-7 and EGFP-8, which contain NLS-1 in combination with NLS-4 or NLS-3 and NLS-4, respectively, showed fluorescence patterns similar to that of EGFP-5 (Figs. 8K and 8L). Confocal microscopy showed localization of fluorescence from EGFP-7 and EGFP-8 in both the nucleus and the nucleolus (Figs. 9E and 9F).

However, EGFP-6, which contains NLS-1, NLS-2, and NLS-3, but not NLS-4, showed nuclear fluorescence (Fig. 8J). As with EGFP-7 and EGFP-8, confocal micro-scropy of EGFP-6 showed localization of fluorescence to the nucleus and nucleolus (Fig. 9F). Interestingly, when the amino-terminal portion of DENTT that includes NLS-1 was deleted to generate the construct EGFP-9 containing NLS-2, NLS-3, and NLS-4 (Fig. 7) nuclear fluorescence was exhibited, but fluorescence was excluded from the nucleolus (Fig. 8M). EGFP-10 was made by deletion of NLS-1 and NLS-2 so that only the region containing NLS-3 and NLS-4 remained (Fig. 7). Figure 8N shows that transfection of EGFP-10 into

FIG. 9. Subcellular localization of fusion proteins containing EGFP linked to portions of the DENTT protein using confocal microscopy. COS-7 cells were transfected with EGFP fused to (**A**) DENTT (aa 1–340) = EGFP-1; (**B**) DENTT (aa 144–347) = EGFP-2; (**C**) DENTT (aa 1–347) = EGFP-5; (**D**) DENTT (aa 1–626) = EGFP-6; (**E**) DENTT (aa 1–340, 356–633) = EGFP-7; (**F**) DENTT (aa 1–340, 351–633) = EGFP-8. Representative COS7 cells from transient transfections were photographed using confocal microscopy, and greater than 95% of transfected cells showed representative subcellular localization. Results are representative of three independent experiments.

COS-7 cells yielded a pattern of fluorescence similar to that of EGFP-9, with prominent fluorescence in the nucleus and exclusion from the nucleolus; in addition, EGFP-10 showed localization of fluorescence in the cytoplasm. As a negative control, transiently transfected COS-7 cells expressing only the 27-kDa EGFP protein exhibited fluorescence distributed between the nucleus and the cytoplasm (Fig. 8O), in agreement with results reported in other cell lines (Kain *et al.,* 1995). This distribution of EGFP between the nucleus and the cytoplasm presumably occurs because of the small size of the EGFP protein, which allows it to move freely through the nuclear pores (Jans and Hubner 1996; Schlenstedt 1996; Gorlich and Mattaj 1996). As a positive control, transfection of the EGFP/SV40 large T-antigen monopartite NLS fusion protein (Healy *et al.,* 1999) into COS-7 cells showed nuclear fluorescence as previously reported (Fig. 8P). Immunofluorescence microscopy revealed that the transiently transfected EGFP-tagged DENTT constructs colocalized with DNA as demonstrated by the DAPI staining patterns shown in Figs. 8B, 8D, and 8F. Nontransfected cells were evident by their lack of staining for EGFP and positive staining for DNA with DAPI.

DISCUSSION

TGF-β mediates its mutifunctional effects by eliciting transcriptional responses on numerous target genes that have been identified in recent years. The responsive elements in the promoters of some of these genes have been mapped, and some interacting transcription factors have been identified. For example, TGF-β has been reported to induce potently transcription of plasminogen activator, plasminogen activator inhibitor-1, and itself (Laiho *et al.,* 1986; Keski-Oja *et al.,* 1988a,b; Van Obbergehen-Schilling *et al.,* 1988; Keeton *et al.,* 1991; Jakowlew *et al.,* 1997). It is probable there are other target genes of TGF-β, including genes that have been already cloned and characterized, and genes that have not yet been identified, whose transcription may be affected by TGF-β that may be important in the cellular processes of normal and tumor epithelial cells.

In this report, we describe the isolation and characterization of a novel human cDNA that we have named DENTT, whose expression is modulated by TGF-β1. Previously, we have reported that NCI-H727 cells are responsive to TGF-β1. NCI-H727 cells showed an in-

crease in expression of TGF-β1 mRNA within 6 to 24 h after exposure to TGF-β1, and we have also shown that anchorage-independent growth of these cells in soft agarose is inhibited by TGF-β1 (Jakowlew et al., 1995). Thus, we have continued to utilize NCI-H727 cells as a model system for epithelial cancer and have used differential mRNA display to identify target genes of TGF-β1 in these cells. Because we were interested in identifying target genes of TGF-β1 that may be involved in the induction and/or maintenance of TGF-β-mediated cellular functions rather than immediate-early genes, the treatment of NCI-H727 cells with TGF-β1 was conducted for 24 h. Differential mRNA display showed that expression of several cDNA fragments was potentially regulated by TGF-β1. Northern blot analysis was used to confirm that the cDNA fragment identified by differential mRNA display represented a mRNA whose steady-state level of expression changed as a result of exposure to TGF-β1.

Our study shows that expression of DENTT mRNA is modulated by TGF-β1 in NSCLC cell lines that are responsive to exogenous TGF-β1. In three of four NSCLC cell lines tested, including NCI-H157, NCI-H727, and NCI-H1299, expression of DENTT mRNA was elevated after addition of TGF-β1. In these same cell lines, expression of TGF-β1 mRNA was also elevated in response to TGF-β1 (Jakowlew et al., 1995). In contrast, DENTT and TGF-β1 mRNA expression was not affected by TGF-β1 addition to NCI-H838 cells. We have previously reported that addition of TGF-β1 inhibits the anchorage-independent growth of NCI-H157, NCI-H727, and NCI-H1299 cells in soft agarose, while anchorage-independent growth of NCI-H838 cells is not affected (Jakowlew et al., 1995). We have also examined cell anchorage-independent growth in five additional carcinoid NSCLC cell lines that show a less than 1.2-fold increase in DENTT mRNA in response to TGF-β1. Addition of TGF-β1 to the carcinoid NSCLC cell lines NCI-H679, NCI-H720, NCI-H835, NCI-H1435, and NCI-H1734 did not inhibit their anchorage-independent growth in soft agarose (data not shown). Thus, our data show that induction of DENTT mRNA by TGF-β1 correlates with induction of TGF-β1 mRNA and with inhibition of anchorage-independent growth of NSCLC cells by TGF-β1. Future studies utilizing antisense DENTT oligonucleotides will be needed to determine whether DENTT is directly involved in inhibition of anchorage-independent growth of NCI-H727 cells and other cells. In addition, future studies will be performed to determine whether DENTT is an immediate-early target of TGF-β1.

In addition to NSCLC cells, we have demonstrated that DENTT mRNA can be detected in a variety of normal human tissues, with the highest level of expression in brain and testis. This suggests that DENTT may play a role in normal cell function. Recently, gene expression of SCLC was profiled and compared to that of pulmonary carcinoids and NHBE cells using high-density cDNA arrays. While the overall expression pro-

files of SCLC cells and tumors were shown to be similar to those of NHBE cells, the expression profiles of SCLC tumors and NHBE cells were found to be very different from those of carcinoid tumors (Anbazhagan et al., 1999). Instead, gene expression profiles showed that carcinoids were more related to neural crest-derived brain tumors. In particular, carcinoid tumors were shown to have a high degree of similarity to two types of glial brain cancer, oligodendroglioma and high-grade astrocytoma. Glial cells are thought to be derived from neural crest cells, as are the Kulchinstky cells of the bronchi (Nakielny and Dreyfuss, 1999). Since we isolated DENTT from NCI-H727, a pulmonary carcinoid cell line, and since we see a high level of expression of DENTT mRNA in normal brain, these observations also support an association between the carcinoid cell line and the normal brain tissue. Future studies will be needed to examine expression of DENTT in neural crest-derived brain tumors and their derived cell lines and to determine the possible role that DENTT may play in these cancers.

The identification of a conserved 191-amino-acid domain in DENTT that identifies and defines the TTSN protein superfamily suggests that DENTT may be a new member of this family. The TTSN gene family has been identified only recently, and the function of each member has become known gradually through biochemical and genetic studies. For example, in addition to its high affinity for histones and its well-documented in vitro nucleosome assembly activity (Ishimi et al., 1987; Fujii-Nakata et al., 1992), the yeast NAP-1 homologue has been reported to interact specifically with B-type cyclin Clb2 and to mediate normal mitotic functions in fission yeast and suppress polar bud growth in budding yeast (Kellogg et al., 1995; Kellogg and Murray 1995). The SET protein is homologous to NAP-1 and also interacts specifically with B-type cyclins (Von Lindern et al., 1992). The cyclin B/p34^{cdc2} complex is the kinase that controls the transition between the S phase and the G2 phase in the cell cycle (Norbury and Nurse, 1992). Binding of cyclin B to Cdc2 induces phosphorylation of the complex, which leads to its activation at the G2 to M transition (Cutz, 1982; Enoch and Nurse, 1990). Interestingly, human cyclin B2 has been recently identified to be a direct physical partner of TGF-β RII (Liu et al., 1999). Cdc2 was demonstrated to interact indirectly with TGF-β RII via cyclin B2. It has been postulated that TGF-β may utilize this pathway to arrest cells at the G1 to S transition by inactivating cyclin B/Cdc2, which is required for exiting from the G1/S phase and entering the G2/M phase (Liu et al., 1999). Members of the TTSN family are localized to the nucleus and cytoplasm, are shown to bind cyclinB, and are thought to play a regulatory role in cell proliferation and/or meiotic differentiation. Since DENTT may be a new member of the TTSN superfamily, DENTT may also have a role in cell proliferation or meiotic differentiation. Future experiments using immunoprecipitation with specific antibodies and the yeast two-

hybrid library screening method will be required to determine whether DENTT also interacts with such proteins as TGF-β RII and cyclin B2 or with other proteins.

The open reading frame of DENTT predicts a nuclear protein with two coiled-coil regions. Nuclear proteins have important roles in a variety of processes, including transcription, mRNA processing, replication, and chromosomal organization. Nuclear proteins have intrinsic signals that control active transport across nuclear pore complexes. These signals, known as NLSs and nuclear export signals (NES), have been identified in a variety of nuclear proteins and work in concert with their cognate transport factors that include the family of karypherins (reviewed in Scheer and Weisenberger, 1994). Full-length DENTT contains one potential bipartite NLS and three monopartite NLSs. No NES are predicted to be in DENTT. Using EGFP fused to full-length DENTT and transfected into COS-7 cells, we have demonstrated that DENTT localizes to the nucleolus and the cytoplasm. To determine whether one or more NLSs were needed for nucleolar localization, the subcellular localization pattern of each NLS alone was studied. EGFP constructs containing NLS-1 showed nuclear and cytoplasmic staining. NLS-2 and NLS-3 sequences resemble that of mating type II α (Kalderon *et al.,* 1984), and each EGFP construct showed a speckled nuclear staining pattern. In contrast, the NLS-4 sequence resembles that of SV40 large T-antigen (Kalderon *et al.,* 1984), and the EGFP construct was evenly distributed in the nucleus and was distinctly excluded from the nucleolus. These differences in staining patterns may be due to differences in the composition of the NLS sequences, may reflect varying efficiencies of nuclear transport into the nucleus, or may reflect other unidentified protein sequences required for proper localization to the nucleolus that were disrupted in the truncated EGFP–DENTT constructs.

NLS-1 in combination with either NLS-2 or NLS-4 shows localization to the nucleolus. NLS-1 appears to be necessary for localization of DENTT to the nucleolus because EGFP constructs lacking NLS1 (EGFP-9 and EGFP-10) are localized to the nucleus, but are excluded from the nucleolus. However, NLS-1 is not sufficient for sole localization of DENTT to the nucleolus, since EGFP-1, which contains only NLS-1, shows localization to the nucleus as well. The nucleolus is the main site of ribosome biosynthesis and is also the locus where several viral core proteins transiently accumulate during viral replication (Hatanaka, 1991; Johnson *et al.,* 1998). In addition, it has been proposed that the nucleolus is a critical site of cellular aging (Quaye *et al.,* 1996). Also, no known RNA-binding motifs such as the ribonucleoprotein motif (Burd and Dreyfuss, 1994) were found in DENTT. A number of possible sequence requirements for nucleolar localization have been reported for several proteins, including ribosomal proteins L31 and L5, viral proteins Tat and Rev of the

human immunodeficiency virus, nucleolin, nucleophosmin, and the transcription factor mUBF (Johnson *et al.,* 1998; Michael and Dreyfuss, 1996; Lapeyre *et al.,* 1987; Chan *et al.,* 1989; Maeda *et al.,* 1992). However, no consensus motifs for nucleolar localization have been identified thus far, and the mechanisms of nucleolar localization are unclear. Studies to identify other DENTT interacting proteins will need to be performed to gain insight into the role of DENTT in the nucleus and nucleolus.

In recent years, several novel nuclear genes have been identified using a variety of methods. During the cloning and characterization of DENTT, genes encoding nuclear localization signals have been identified. In one such report, an engineered nuclear export signal-containing transcription factor that is excluded from the nucleus was used with a reporter gene to provide a selection process in yeast to identify and enrich for cDNAs encoding nuclear targeted proteins. Using this nuclear transportation trap system (NTT), a number of previously reported and novel nuclear localized proteins were identified. The nucleotide sequence of one of the nuclear localized proteins that was identified using the NTT system was compared to DENTT and showed identity (Ueki *et al.,* 1998). The only reported characterization of this nuclear localized protein concerned its localization to the nucleus. The nucleotide sequence of this nuclear localized protein (GenBank Accession No. BAA34802) was identical to DENTT, but lacked the first 600 nucleotides corresponding to 147 amino acids at the amino terminus of DENTT. Because the bipartite NLS of DENTT is located within the initial 142 amino acids of the DENTT protein, NLS-1 was missing from this initial report (Ueki *et al.,* 1998). Since the region of DENTT containing NLS-1 is an important component for localization of DENTT to the nucleolus, its absence explains the lack of nucleolar localization of this shorter DENTT. Our study clearly shows that DENTT localizes to the nucleolus and cytoplasm and that NLS-1 is required for nucleolar localization. Our data suggest that this novel TGF-β1 target gene has distinct domains for direction of the protein to different subnuclear locations. Additional studies will be required to characterize the role DENTT plays in the nucleolus and to determine the role that DENTT plays as a target gene of TGF-β1. Moreover, it will be important to determine whether DENTT has a role in TGF-β1-mediated inhibition of anchorage-independent growth.

REFERENCES

Adachi, Y., Pavlakis, G. N., and Copeland, T. D. (1994). Identification and characterization of SET, a nuclear phosphoprotein encoded by the translocation break point in acute undifferentiated leukemia. *J. Biol. Chem.* **269:** 2258–2262.

Anbazhagan, R., Tihan, T., Bornman, D. M., Johnston, J. C., Saltz, J. H., Weigering, A., Piantadosi, S., and Gabrielson, E. (1999). Classification of small cell lung cancer and pulmonary carcinoid by gene expression profiles. *Cancer Res.* **59:** 5119–5122.

Burd, C. G., and Dreyfuss, G. (1994). Conserved structures and diversity of functions of RNA-binding proteins. *Science* **265:** 615–621.

Carbone, D., and Kratzke, R. (1996). Cancer of the lung. *In* "Lung Cancer: Principles and Practice" (J. Mitchell, D. Johnson, and A. Turrisi, Eds.), pp. 107–121, Lippencott-Raven, Philadelphia.

Chan, W. Y., Liu, Q. R., Borjigin, J., Busch, H., Rennart, O. M., Tease, L. A., and Chan, P. K. (1989). Characterization of the cDNA encoding human nucleophosmin and studies of its role in normal and abnormal growth. *Biochemistry* **28:** 1033–1039.

Chen, R. H., Miettinen, P. J., Maruoka, E. M., Choy, L., and Derynck, R. (1995). A WD-domain protein that is associated with and phosphorylated by the type II TGF-beta receptor. *Nature* **377:** 548–552.

Chen, Y-G., Liu, F., and Massague, J. (1997). Mechanism of TGFβ receptor inhibition by FKBP12. *EMBO J.* **16:** 3866–3876.

Chirgwin, J. M., Przybyla, A. E., MacDonald, R. J., and Rutter, W. J. (1979). Isolation of biologically active ribonucleic acid from sources enriched in ribonuclease. *Biochemistry* **18:** 5294–5299.

Church, G. M., and Gilbert, W. (1984). Genomic sequencing. *Proc. Natl. Acad. Sci. USA* **81:** 1991–1995.

Cutz, E. (1982). Neuroendocrine cells of the lung: An overview of morphologic characteristics and development. *Exp. Cell Res.* **3:** 185–208.

Derynck, R., and Choy, L. (1998). Transforming growth factor-β and its receptors. *In* "The Cytokine Handbook" (A. W. Thomsom, Ed.), pp. 593–636, Academic Press, San Diego.

Dingwall, C., and Laskey, R. A. (1991). Nuclear targeting sequences—A consensus? *Trends Biochem. Sci.* **16:** 478–481.

Enoch, T., and Nurse, P. (1990). Mutation of fission yeast cell cycle control genes abolishes dependence of mitosis on DNA replication. *Cell* **60:** 665–673.

Fitzgerald, M., and Shenk, T. (1981). The sequence 5′-AAUAAA-3′ forms parts of the recognition site for polyadenylation of late SV40 mRNAs. *Cell* **24:** 251–260.

Fujii-Nakata, T., Ishimi, Y., Okuda, A., and Kikuchi, A. (1992). Functional analysis of nucleosome assembly protein, NAP-1. The negatively charged COOH-terminal region is not necessary for the intrinsic assembly activity. *J. Biol. Chem.* **267:** 20980–20986.

Ginsberg, R. J. (1993). Multimodality therapy for stage IIIA (N2) lung cancer: An overview. *Chest* **103:** 356s–359s.

Gorlich, D., and Mattaj, I. W. (1996). Nucleocytoplasmic transport. *Science* **271:** 1513–1518.

Hatanaka, M. (1991). Nucleolar targeting signals (NOS) of HIV. *In* "Genetic Structure and Regulation of HIV" (W. A. Haseltine and F. Wong-Staal, Eds.), pp. 264–287, Raven Press, New York.

Hayashi, H., Abdollah, S., Qiu, Y., Cai, J., Xu, Y. Y., Grinnell, B. W., Richardson, M. A., Topper, J. N., Gimbrone, Jr., M. A., Wrana, J. L., and Falb, D. (1997). The MAD-related protein Smad7 associates with the TGFbeta receptor and functions as an antagonist of TGFbeta signaling. *Cell* **89:** 1165–1173.

Healy, A. M., Peters-Golden, M., Yao, J. P., and Brock, T. G. (1999). Identification of a bipartite nuclear localization sequence necessary for nuclear import of 5-lipoxygenase. *J. Biol. Chem.* **274:** 29812–29819.

Heldin C-H., Miyazono, K., and ten Dijke, P. (1997). TGF-beta signalling from cell membrane to nucleus through SMAD proteins. *Nature* **390:** 465–471.

Imamura, T., Takase, M., Nishihara, A., Oeda, E., Hanai, J., Kawabata, M., and Miyazono, K. (1997). Smad6 inhibits signalling by the TGF-beta superfamily. *Nature* **389:** 622–626.

Ishimi, Y., Hirosumi, J., Sato, W., Sugasawa, K., Yokota, S., Hanaoka, F., and Yamada, M. (1984). Purification and initial characterization of a protein which facilitates assembly of nucleosome-like structure from mammalian cells. *Eur. J. Biochem.* **142:** 431–439.

Ishimi, Y., Kojima, M., Yamada, M., and Hanaoka, F. (1987). Binding mode of nucleosome-assembly protein (AP-I) and histones. *Eur. J. Biochem.* **162:** 19–24.

Ishimi, Y., and Kikuchi, A. (1991). Identification and molecular cloning of yeast homolog of nucleosome assembly protein I which facilitates nucleosome assembly in vitro. *J. Biol. Chem.* **266:** 7025–7029.

Jakowlew, S. B., Mathias, A., Chung, P., and Moody, T. W. (1995). Expression of transforming growth factor beta ligand and receptor messenger RNAs in lung cancer cell lines. *Cell Growth Differ.* **6:** 465–476.

Jakowlew, S. B., Mariano, J. M., You, L., and Mathias, A. (1997). Differential regulation of protease and extracellular matrix protein expression by transforming growth factor-beta 1 in non-small cell lung cancer cells and normal human bronchial epithelial cells. *Biochim. Biophys. Acta* **1353:** 157–170.

Jans, D. A., and Hubner, S. (1996). Regulation of protein transport to the nucleus: Central role of phosphorylation. *Physiol. Rev.* **76:** 651–685.

Johnson, F. B., Marciniak, R. A., and Guarente, L. (1998). Telomeres, the nucleolus and aging. *Curr. Opin. Cell. Biol.* **10:** 332–338.

Kain, S. R., Adams, M., Kondepudi, A., Yang, T. T., Ward, W. W., and Kitts, P. (1995). Green fluorescent protein as a reporter of gene expression and protein localization. *BioTechniques* **19:** 650–655.

Kalderon, D., Richardson, W. D., Markham, A. F., and Smith, A. E. (1984). Sequence requirements for nuclear location of simian virus 40 large-T antigen. *Nature* **311:** 33–38.

Kawabata, M., Imamura, T., Miayazono, K., Engel, M. E., and Moses, H. L. (1995). Interaction of the transforming growth factor-beta type I receptor with farnesyl-protein transferase-alpha. *J. Biol. Chem.* **270:** 29628–29631.

Keeton, M. R., Curriden, S. A., van Zonneveld, A. J., and Loskutoff, D. J. (1991). Identification of regulatory sequences in the type 1 plasminogen activator inhibitor gene responsive to transforming growth factor beta. *J. Biol. Chem.* **266:** 23048–23052.

Kellogg, D. R., Kikuchi, A., Fujii-Nakata, T., Turck, C. W., and Murray, A. W. (1995). Members of the NAP/SET family of proteins interact specifically with B-type cyclins. *J. Cell. Biol.* **130:** 661–673.

Kellogg, D. R., and Murray, A. W. (1995). NAP1 acts with Clb1 to perform mitotic functions and to suppress polar bud growth in budding yeast. *J. Cell. Biol.* **130:** 675–685.

Kern, J., and Filderman, A. (1993). Oncogenes and growth factors in human lung cancer. *Clin. Chest Med.* **14:** 31–41.

Keski-Oja, J., Raghow, R., Sawdey, M., Loskutoff, D. J., Postlewaite, A. E., Kang, A. H., and Moses, H. L. (1988a). Regulation of mRNAs for type-1 plasminogen activator inhibitor, fibronectin, and type I procollagen by transforming growth factor-beta. Divergent responses in lung fibroblasts and carcinoma cells. *J. Biol. Chem.* **263:** 3111–3115.

Keski-Oja, J., Blasi, F., Leof, E. B., and Moses, H. L. (1988b). Regulation of the synthesis and activity of urokinase plasminogen activator in A549 human lung carcinoma cells by transforming growth factor-beta. *J. Cell. Biol.* **106:** 451–459.

Kozak, M. (1981a). Mechanism of mRNA recognition by eukaryotic ribosomes during initiation of protein synthesis. *In* "Current Topics in Microbiology and Immunology" (A. J. Shatkin, Ed.), Vol. 293, pp. 81–123, Springer-Verlag, Berlin.

Kozak, M. (1981b). Possible role of flanking nucleotides in recognition of the AUG initiator codon by eukaryotic ribosomes. *Nucleic Acids Res.* **9:** 5233–5262.

Kozak, M. (1982). Analysis of ribosome binding sites from the s1 message of reovirus. Initiation at the first and second AUG codons. *J. Mol. Biol.* **156:** 807–820.

Laiho, M., Saksela, O., Andreason, P. A., and Keski-Oja, J. (1986). Enhanced production and extracellular deposition of the endothelial-type plasminogen activator inhibitor in cultured human lung fibroblasts by transforming growth factor-beta. *J. Cell. Biol.* **103:** 2403–2410.

Landis, S. H., Murray, T., Bolden, S., and Wingo, P. A, (1999). Cancer statistics 1999. *CA Cancer J. Clin.* **49:** 8–31.

Lapeyre, B., Bourbon, H., and Amalric, F. (1987). Nucleolin, the major nucleolar protein of growing eukaryotic cells: An unusual protein structure revealed by the nucleotide sequence. *Proc. Natl. Acad. Sci. USA* **84:** 1472–1476.

Liang, P., and Pardee, A. B. (1992). Differential display of eukaryotic messenger RNA by means of the polymerase chain reaction. *Science* **257:** 967–971.

Liang, P., Zhu, W., Zhang, X., Guo, Z., O'Connell, R. P., Averboukh, L., Wang, F., and Pardee, A. B. (1994). Differential display using one-base anchored oligo-dT primers. *Nucleic Acids Res.* **22:** 5763–5764.

Liu, J. H., Wei, S., Burnette, P. K., Gamero, A. M., Hutton, M., and Djeu, J. Y. (1999). Functional association of TGF-beta receptor II with cyclin B. *Oncogene* **18:** 269–275.

Maeda, Y., Hisatake, K., Kondo, T., Hanada, K., Song, C. Z., Nishimura, T., and Muramatsu, M. (1992). Mouse rRNA gene transcription factor mUBF requires both HMG-box1 and an acidic tail for nucleolar accumulation: Molecular analysis of the nucleolar targeting mechanism. *EMBO J.* **11:** 3695–3704.

Massague', J. (1998). TGF-beta signal transduction. *Annu. Rev. Biochem.* **67:** 753–791.

Massague' J., Cheifetz, S., Laiho, M., and Ralph, D. A. (1992). Transforming growth factor-beta. *Cancer Surv.* **12:** 81–103.

Michael, W. M., and Dreyfuss, G. (1996). Distinct domians in ribosomal protein L5 mediate 5 S rRNA binding and nucleolar localization. *J. Biol. Chem.* **271:** 11571–11574.

Montell, C., Fisher, E. F., Caruthers, M. H., and Berk, A. J. (1983). Inhibition of RNA cleavage but not polyadenylation by a point mutation in mRNA 3′ consensus sequence AAUAAA. *Nature* **305:** 600–605.

Moses, H. L., Tucker, R. F., Leof, E. B., Coffey, R. J., Halper, J., and Shipley, G. D. (1985). Type β transforming growth factor is a growth stimulator and growth inhibitor. *In* "Cancer Cells, Growth Factors and Transformation" (J. Feramisco, B. Ozane, and C. Stiles, Eds.), Vol. 3, pp. 65–71, Cold Spring Harbor Laboratory Press, Cold Spring Harbor, NY.

Nakielny, S., and Dreyfuss, G. (1999). Transport of proteins and RNAs in and out of the nucleus. *Cell* **99:** 677–690.

Norbury, C., and Nurse, P. (1992). Animal cell cycles and their control. *Annu. Rev. Biochem.* **61:** 441–470.

Pezzella, F., Turley, H., Kuzu, I., Tungekar, M. F., Dunnill, M. S., Pierce, C. B., Harris, A., Gutter, K. C., and Mason, D. Y. (1993). bcl-2 protein in non-small-cell lung carcinoma. *N. Engl. J. Med.* **329:** 690–694.

Prins, J., De Vries, E., and Mulder, N. (1993). The myc family of oncogenes and their presence and importance in small-cell lung carcinoma and other tumour types. *Anticancer Res.* **13:** 1373–1385.

Proudfoot, N. J., and Brownlee, G. G. (1976). 3′ non-coding region sequences in eukaryotic messenger RNA. *Nature* **263:** 211–214.

Qian, S-W., Kondaiah, P., Roberts, A. B., and Sporn, M. B. (1990). cDNA cloning by PCR of rat transforming growth factor beta-1. *Nucleic Acids Res.* **8:** 3059.

Quaye, I. K., Toku, S., and Tanaka, T. (1996). Sequence requirement for nucleolar localization of rat ribosomal protein L31. *Eur. J. Cell. Biol.* **69:** 151–155.

Roberts, A. B., Anzano, M. A., Wakefield, L. M., Roche, N. S., Stern, D. F., and Sporn, M. B. (1985). Type beta transforming growth factor: A bifunctional regulator of cellular growth. *Proc. Natl. Acad. Sci. USA* **82:** 119–123.

Roberts, A. B., and Sporn, M. B. (1990). The transforming growth factor-βs. *In* "Handbook of Experimental Pharmacology" (M. B. Sporn and A. B. Roberts, Eds.), pp. 419–472, Springer-Verlag, Berlin.

Roberts, A. B., Heine, U. I., Flanders, K. C., and Sporn, M. B. (1990). Transforming growth factor-β: Major role in regulation of extracellular matrix. *Ann. N.Y. Acad. Sci.* **580:** 225–232.

Scheer, U., and Weisenberger, D. (1994). The nucleolus. *Curr. Opin. Cell Biol.* **6:** 354–359.

Schlenstedt, G. (1996). Protein import into the nucleus. *FEBS Lett.* **389:** 75–79.

Shapiro, G., Edwards, C., Kobzik, L., Godleski, J., Richards, W., Sugarbaker, D., and Rollins, B. (1995). Reciprocal Rb inactivation and p16INK4 expression in primary lung cancers and cell lines. *Cancer Res.* **55:** 505–509.

Shin, S., Freedman, V. H., Risser, R., and Pollack, R. (1975). Tumorigenicity of virus-transformed cells in nude mice is correlated specifically with anchorage independent growth in vitro. *Proc. Natl. Acad. Sci. USA* **72:** 4435–4439.

Sidransky, D., and Hollstein, M. (1996). Clinical implications of the p53 gene. *Annu. Rev. Med.* **47:** 285–301.

Slebos, R., and Rodenhuis, S. (1992). The ras gene family in human non-small-cell lung cancer. *J. Natl. Cancer. Inst.* **13:** 23–29.

Tyler-Smith, C., Taylor, L., and Muller, U. (1988). Structure of a hypervariable tandemly repeated DNA sequence on the short arm of the human Y chromosome. *J. Mol. Biol.* **203:** 837–848.

Ueki, N., Oda, T., Kondo, M., Yano, K., Noguchi, T., and Muramatsu, M. (1998). Selection system for genes encoding nuclear-targeted proteins. *Nat. Biotech.* **16:** 1338–1342.

Van Obbergehen-Schilling, E., Roche, N. S., Flanders, K. C., Sporn, M. B., and Roberts, A. B. (1988). Transforming growth factor beta 1 positively regulates its own expression in normal and transformed cells. *J. Biol. Chem.* **263:** 7741–7746.

Ventura, F., Liu, F., Doody, J., and Massague', J. (1996). Interaction of transforming growth factor-beta receptor I with farnesyl-protein transferase-alpha in yeast and mammalian cells. *J. Biol. Chem.* **271:** 13931–13934.

Vogel, T., Dittrich, O., Mehraein, Y., Dechend, F., Schnieders, F., and Schmidtke, J. (1998). Murine and human TSPYL genes: Novel members of the TSPY-SET-NAP1L1 family. *Cytogenet. Cell. Genet.* **81:** 265–270.

Von Lindern, M., Van Baal, S., Wiegant, J., Raap, A., Hagemeijer, A., and Grosveld, G. (1992). Can, a putative oncogene associated with myeloid leukemogenesis, may be activated by fusion of its 3′ half to different genes: Characterization of the set gene. *Mol. Cell. Biol.* **12:** 3346–3355.

Wang, T., Donahoe, P. K., and Zervos, A. S. (1994). Specific interaction of type I receptors of the TGF-beta family with the immunophilin FKBP-12. *Science* **265:** 674–676.

Wang, T., Danielson, P. D., Li, B-Y., Shah, P. C., Kim, S. D., and Donahoe, P. K. (1996). The p21(RAS) farnesyltransferase alpha subunit in TGF-beta and activin signaling. *Science* **271:** 1120–1122.

Weissenbach, J., Goodfellow, P. N., and Smith, K. D. (1989). Report of the committee on the genetic constitution of the Y chromosome. *Cytogenet. Cell. Genet.* **51:** 438–449.